Sulfatase modifying factor 1–mediated fibroblast growth factor signaling primes hematopoietic multilineage development

Mario Buono,[1] Ilaria Visigalli,[2] Roberta Bergamasco,[1] Alessandra Biffi,[2] and Maria Pia Cosma[1,3]

[1]Telethon Institute of Genetics and Medicine, 80134 Naples, Italy
[2]San Raffaele Telethon Institute for Gene Therapy, Division of Regenerative Medicine, San Raffaele Scientific Institute, 20132 Milan, Italy
[3]Institute of Genetics and Biophysics, National Research Council of Italy, 80131 Naples, Italy

Self-renewal and differentiation of hematopoietic stem cells (HSCs) are balanced by the concerted activities of the fibroblast growth factor (FGF), Wnt, and Notch pathways, which are tuned by enzyme-mediated remodeling of heparan sulfate proteoglycans (HSPGs). Sulfatase modifying factor 1 (SUMF1) activates the Sulf1 and Sulf2 sulfatases that remodel the HSPGs, and is mutated in patients with multiple sulfatase deficiency. Here, we show that the FGF signaling pathway is constitutively activated in *Sumf1*$^{-/-}$ HSCs and hematopoietic stem progenitor cells (HSPCs). These cells show increased p-extracellular signal-regulated kinase levels, which in turn promote β-catenin accumulation. Constitutive activation of FGF signaling results in a block in erythroid differentiation at the chromatophilic erythroblast stage, and of B lymphocyte differentiation at the pro–B cell stage. A reduction in mature myeloid cells and an aberrant development of T lymphocytes are also seen. These defects are rescued in vivo by blocking the FGF pathway in *Sumf1*$^{-/-}$ mice. Transplantation of *Sumf1*$^{-/-}$ HSPCs into wild-type mice reconstituted the phenotype of the donors, suggesting a cell autonomous defect. These data indicate that Sumf1 controls HSPC differentiation and hematopoietic lineage development through FGF and Wnt signaling.

CORRESPONDENCE
Alessandra Biffi:
biffi.alessandra@hsr.it
OR
Maria Pia Cosma:
cosma@tigem.it

Abbreviations used: APC, adenomatous polyposis coli; CFU-E, erythroid CFU; CFU-GM, myeloid CFU; CLP, common lymphoid progenitor; CMP, common myeloid progenitor; DP, double positive; ERK, extracellular signal-regulated kinase; FGF, fibroblast growth factor; GMP, granulocyte–monocyte progenitor; GSK, glycogen synthase kinase; HSC, hematopoietic stem cell; HSPC, hematopoietic stem progenitor cell; HSPGs, heparan sulfate proteoglycans; KLS, c-kit$^+$, lineage−, and Sca1$^+$; LT-HSC, long-term HSC; LV, lentivirus; MEP, megakaryocyte–erythrocyte progenitor; MPP, multipotent progenitor; MSD, multiple sulfatase deficiency; SP, single positive; ST-HSC, short-term HSC; SUMF1, sulfatase modifying factor 1.

To catalyze the hydrolysis of their natural substrates, sulfatases must be posttranslationally activated. A consensus sequence in their catalytic domain contains a cysteine that is modified into formylglycine by the formylglycine-generating enzyme encoded by the *sulfatase modifying factor 1* (*SUMF1*) gene (Schmidt et al., 1995; Cosma et al., 2003; Dierks et al., 2003). SUMF1 exerts its activity within the ER; however, it can also be secreted and taken up by distant cells and tissues, where it relocalizes in the ER as an active enzyme (Zito et al., 2007). Multiple sulfatase deficiency (MSD) is a human monogenic disorder in which all of the sulfatase activities are simultaneously defective (Hopwood and Ballabio, 2001). Patients with MSD have mutations in *SUMF1* (Cosma et al., 2004). A *Sumf1*$^{-/-}$ strain has been generated as a mouse model of MSD, and it shows a complete loss of sulfatase activities, early mortality, congenital growth retardation, skeletal abnormalities, neurological defects, and a generalized inflammatory process in many organs (Settembre et al., 2007).

These *Sumf1*$^{-/-}$ mice represent an important resource to study developmental defects associated with SUMF1 lack of function. Indeed, SUMF1 also has putative activity during development specification. To date, 17 different sulfatases have been described in humans, and all are activated by SUMF1 (Sardiello et al., 2005). Among this large sulfatase family, Sulf1 and Sulf2 are localized on the cell surface and catalyze hydrolysis of the 6-*O*-sulfate of the N-acetyl glucosamines of heparan during degradation of heparan sulfate proteoglycans (HSPGs; Morimoto-Tomita et al., 2002). Wingless

M.P. Cosma's present address is the Center for Genomic Regulation, E-08003 Barcelona, Spain.

The Rockefeller University Press $30.00
J. Exp. Med. Vol. 207 No. 8 1647-1660
www.jem.org/cgi/doi/10.1084/jem.20091022

(Wg)/Wnt belongs to a family of secreted morphogenic proteins that control tissue-specific cell fate decisions during embryogenesis, and that bind to the heparan sulfate moieties on the cell surface of HSPGs (Logan and Nusse, 2004; Bejsovec, 2005). QSulf, the avian orthologue of human Sulf (hSulf), removes the sulfate from heparan sulfate, and releases Wnt from HSPGs. This released Wnt associates with Frizzled (Fz) and LRP5/6 receptors, resulting in inactivation of a multiprotein destruction complex, which is composed of glycogen synthase kinase-3 (GSK-3), *Axin2*, and adenomatous polyposis coli (APC). This inactivation leads to translocation of β-catenin into the nucleus, where it activates several target genes (Hoppler and Kavanagh, 2007). In addition to its role in embryogenesis, Wnt is involved in controlling proliferation of stem cells. Wnt3a belongs to the Wnt family, and has been shown to enhance self-renewal and maintain totipotency/multipotency of embryonic stem cells and hematopoietic stem cells (HSCs), respectively, through accumulation of β-catenin in the cell nucleus (Reya et al., 2003; Anton et al., 2007). Furthermore, transplantation of Wnt3a-treated BM increases the survival of lethally irradiated mice (Willert et al., 2003).

HSCs reside in the BM and are a rare population of adult pluripotent stem cells that have the dual capability of self-renewal and differentiation into all blood cell lineages. Based on their ability to self-renew, HSCs can be defined as long-term (LT-HSCs) and short-term (ST-HSCs) HSCs. LT-HSCs have extensive self-renewal abilities and sustain life-long hematopoiesis, whereas ST-HSCs represent a more committed population with short self-renewal potential (Laiosa et al., 2006a). That Wnt signaling stimulates proliferation and self-renewal of HSCs was suggested >10 yr ago (Austin et al., 1997). More recently, it has been shown that exposure of HSCs to Wnt antagonists in vitro reduces their proliferation ability and that Bcl-2 transgenic HSCs transduced with retroviral vectors encoding β-catenin can fully reconstitute the hematopoietic compartments of recipients (Reya et al., 2003). On the other hand, stable expression of β-catenin from the Rosa26 locus in transgenic mice led to loss of HSC repopulation and multilineage differentiation potential (Kirstetter et al., 2006). Mice with β-catenin deletion in their HSCs show normal hematopoiesis (Cobas et al., 2004). These apparently contradictory data might reveal some novel aspects of the function of the Wnt signaling pathway. Indeed, it appears that different and specific amounts of β-catenin confer divergent phenotypes and differentiation capabilities to HSCs.

In addition, a fine-tuned balance between different signaling pathways might be important to control self-renewal and differentiation of HSCs. The Notch and Wnt pathways have been shown to act in synergy to maintain the HSC pool, with Wnt being important to induce proliferation and support viability of HSCs, and Notch being important in the maintenance of HSCs in an undifferentiated state (Duncan et al., 2005). Furthermore, in vivo inhibition of GSK-3β augments the repopulation abilities of transplanted HSCs via modulation of gene targets of both the Wnt and Notch pathways (Trowbridge et al., 2006).

Interestingly, the activities of Sulf1 and Sulf2 modulate Wnt signaling by modifying the sulfation state of the heparan sulfates contained in HSPGs, thereby impairing fibroblast growth factor (FGF) signaling. Crystal structure studies have demonstrated that binding of FGF1 and FGF2 to the FGF receptor is stabilized by 6-*O*-sulfation of the heparan sulfates of the HSPGs (Pellegrini et al., 2000). Thus, through desulfation of these heparan sulfates, hSulf1 can down-regulate FGF-dependent extracellular signal-regulated kinase (ERK) kinase activity (Lai et al., 2003). FGF1 and FGF2 signaling preserves ex vivo expansion of primitive HSCs (Yeoh et al., 2006).

Thus, an intriguing question is raised: does Sumf1 act as a master regulator of the signaling of the Wnt and FGF pathways through activation of Sulf1 and/or Sulf2, resulting, in turn, in modulation of developmental signals and of HSC self-renewal and cell lineage commitment?

Here, we show that SUMF1 has a role in promoting cell lineage commitment. *Sumf1*$^{-/-}$ HSCs and hematopoietic stem progenitor cells (HSPCs) show constitutive activation of the FGF signaling pathway, and the consequent increase in p-ERK leads to GSK3-β phosphorylation and β-catenin accumulation. In turn, Notch is also accumulated. These altered signaling pathways lead to a block of erythroid, myeloid, and lymphoid differentiation in *Sumf1*$^{-/-}$ mice. We also provide evidence that *Sulf2*$^{-/-}$ mice recapitulates the *Sumf1*$^{-/-}$ BM phenotype up to a certain point. In contrast, *Ids*$^{-/-}$ and *Sgsh*$^{-/-}$ mice, which are two mouse loss-of-function sulfatase models, did not show any relevant hematopoietic differentiation defects. Furthermore, upon transplantation of *Sumf1*$^{-/-}$ HSPCs into lethally irradiated WT mice, there was impaired differentiation of the donor cells, which recapitulates the hematopoietic defects seen in the *Sumf1*$^{-/-}$ mice; furthermore, in the recipient mice, a decrease in the frequency of LT-HSCs was observed. These findings confirm that the differentiation impairment of the mutant HSCs and their progeny is caused by SUMF1 loss of function, and not by different environmental features.

RESULTS

FGF and canonical Wnt signaling pathways are constitutively activated in HSPCs of *Sumf1*$^{-/-}$ mice

HSC differentiation and self-renewal are modulated by different mitotic stimuli. Thus, we analyzed whether the Wnt–β-catenin and FGF signaling pathways are altered in HSPCs from *Sumf1*$^{-/-}$ mice. The HSPCs were purified from the BM of 3-wk-old *Sumf1*$^{-/-}$ mice, and from age-matched WT mice, by lineage-negative selection. Sulf1 and Sulf2 activities were fully impaired in homogenates of *Sumf1*$^{-/-}$ HSPCs (Fig. 1 A). Sulf1 and Sulf2 inactivation leads to an increase in the signaling of FGF, which is caused by stabilization of the HSPG–FGFR–FGF trimeric complex (Wang et al., 2004; Lamanna et al., 2008). Indeed, there was also increased phosphorylation of ERK, a downstream effector of FGF signaling,

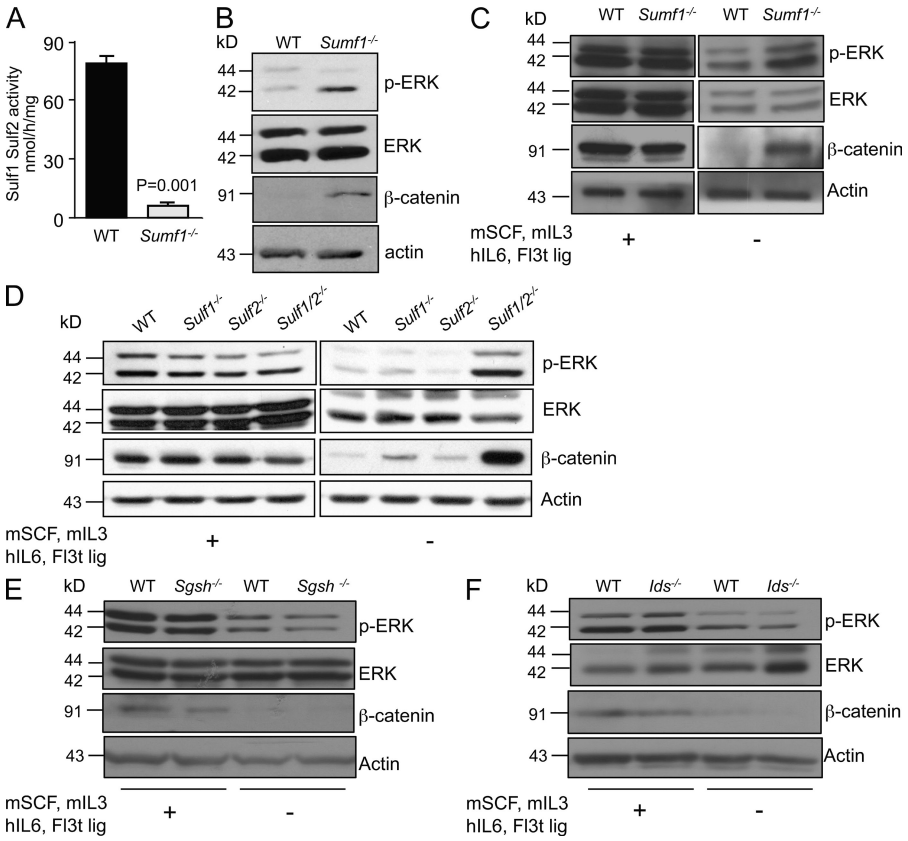

Figure 1. Constitutive activation of FGF and Wnt signaling in *Sumf1*$^{-/-}$ HSPCs. (A) Sulf1 and Sulf2 enzymatic activities in total homogenates of WT and *Sumf1*$^{-/-}$ HSPCs. The activities are reported as nanomole/hour/milligram protein, as indicated (means ± SD; $n = 3$). (B–F) Western blots with the indicated antibodies of total homogenates from freshly isolated WT and *Sumf1*$^{-/-}$ HSPCs (B); cultured WT and *Sumf1*$^{-/-}$ HSPCs (C); WT, *Sulf1*$^{-/-}$, *Sulf2*$^{-/-}$, and *Sulf1/2* double-KO HSPCs (D); WT and *Sgsh*$^{-/-}$ HSPCs (E); and WT and *Ids*$^{-/-}$ HSPCs (F). Data are representative of three independent experiments ($n = 3$ for each mouse model). Cells were cultured or not with recombinant cytokines, as indicated. The loading controls were anti-actin and anti-ERK1/ERK2.

both in freshly isolated *Sumf1*$^{-/-}$ HSPCs (Fig. 1 B) and in *Sumf1*$^{-/-}$ HSPCs cultured without growth-factor stimulation (Fig. 1 C, right). As expected, no differences were seen when the cells were cultured in an enriched medium, because the added growth factors can themselves modulate several signaling pathways (Fig. 1 C, left). The FGF signaling pathway was specifically activated in the *Sumf1*$^{-/-}$ HSPCs because there was increased phosphorylation of the downstream effector FSR2 (Kouhara et al., 1997) and increased transcription of *GPC3*, which positively modulates the pathway (Lai et al., 2008; Fig. S1, A and B).

Surprisingly, accumulation of β-catenin was seen in both freshly isolated and cultured *Sumf1*$^{-/-}$ HSPCs (Fig. 1, B and C, right). This was not expected; indeed, inactivation of Sulf1 and Sulf2 should result in the inactivation of the canonical Wnt pathway, with the consequent β-catenin degradation (Ai et al., 2003). The accumulation of β-catenin and the increase in ERK phosphorylation were specifically caused by inactivation of both Sulf1 and Sulf2 in the *Sumf1*$^{-/-}$ HSPCs, as confirmed by the analysis with HSPCs isolated from the BM of *Sulf1*$^{-/-}$ *Sulf2*$^{-/-}$ double-KO mice (Fig. 1 D, left). In contrast, there were no differences in the levels of p-ERK and in β-catenin accumulation in retrieved HSPCs from the BM of MPSIIIA (deficient in SGSH sulfatase) and MPSII (deficient in IDS sulfatase) mice, as compared with WT mice (Fig. 1, E and F), thus excluding a role of the other sulfatases.

To demonstrate the constitutive activation of FGF and Wnt signaling in HSCs, the c-kit$^+$, lineage$^-$, and Sca1$^+$ (KLS) cell fraction of HSPCs was purified from WT and *Sumf1*$^{-/-}$ mice. These KLS cells were then transduced with lentiviruses (LVs) carrying 4X β-catenin or an ERK-responsive element upstream of a minimal CMV promoter controlling enhanced GFP (eGFP) expression. eGFP expression was quantified as percentages of eGFP$^+$ cells within the KLS cells (Fig. 2 A), LT-HSCs (Kit$^+$, Lin$^-$, Sca1$^+$, and CD150$^+$; Fig. 2 B) and ST-HSCs (Kit$^+$, Lin$^-$, Sca1$^+$, and CD150$^-$; Fig. 2 C). The FGF and Wnt/β-catenin pathways were constitutively activated in all of the *Sumf1*$^{-/-}$ cell populations analyzed, as demonstrated by the increased frequency of GFP$^+$ cells in these populations, as compared with their WT counterparts.

Finally, we tested the HSPC clonogenic potential by counting CFUs of WT and *Sumf1*$^{-/-}$ HSPCs obtained with the colony-forming cell assay. Here, 30% less total CFUs were originated by *Sumf1*$^{-/-}$ HSPCs, as compared with WT HSPCs. There were no differences in the morphologies and amounts of erythroid CFUs (CFU-E), but a significant reduction in myeloid CFUs (CFU-GM; Fig. 2 D), although the ratios of both CFU-E and CFU-GM with respect to the total number of colonies was comparable (Fig. 2 E).

These data demonstrate that the FGF and Wnt/β-catenin pathways are constitutively active in HSPCs from *Sumf1*$^{-/-}$ mice, and also it might be possible that SUMF1 modulates these pathways through Sulf1 and Sulf2 activities.

Increased ERK phosphorylation in *Sumf1*$^{-/-}$ HSPCs controls activation of the Wnt–β-catenin signaling pathway

We next asked whether accumulation of β-catenin in *Sumf1*$^{-/-}$ HSPCs is caused by increased phosphorylation of ERK. Inactivation of GSK-3β, the kinase that is part of the β-catenin destruction complex, occurs via its phosphorylation.

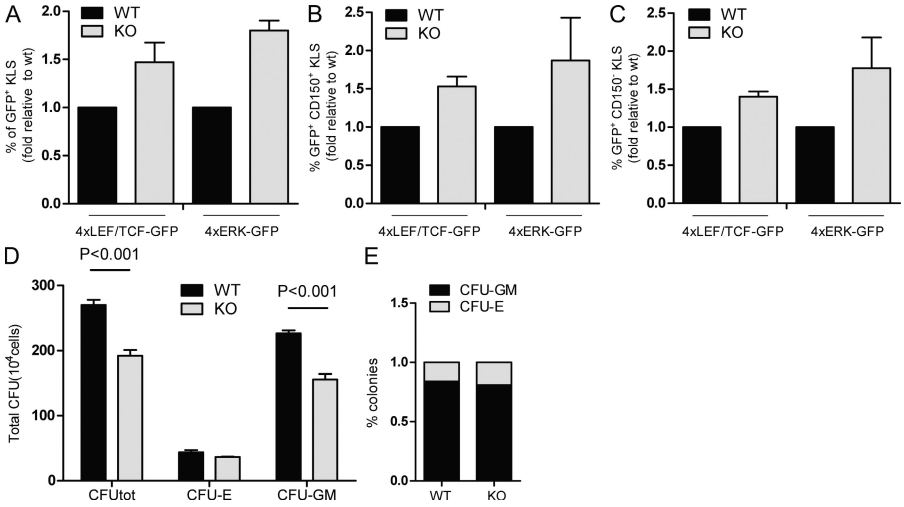

Figure 2. Constitutive activation of FGF and Wnt signaling in the KLS cells of *Sumf1*$^{-/-}$ mice. Percentage of cells expressing β-catenin (LEF/TCF) and ERK GFP reporters in gated *Sumf1*$^{-/-}$ (KO) KLS (Lin$^-$ kit$^+$ Sca1$^+$; A), LT-HSC (Lin$^-$ kit$^+$ Sca1$^+$ CD150$^+$; B), and ST-HSC (Lin$^-$ kit$^+$ Sca1$^+$ CD150$^-$; C) subsets expressed as fold relative to WT. Data are mean ± SE of three independent experiments (n = 3 for each group with technical triplicates). (D) WT and KO HSPC colony assays, analyzed as total CFU (CFUtot), erythroid CFU (CFU-E), and myeloid CFU (CFU-GM). Data are mean ± SE of three independent experiments (n = 3 for each group with technical triplicates). (E) WT and KO CFU-E and CFU-GM, as percentages of total CFUs.

Although this can be mediated by activation of the canonical Wnt pathway, it can be mediated also by p-ERK (Ding et al., 2005). We tested for the latter possibility by inhibiting p-ERK with the MEK1/2 inhibitor UO126 (Fig. 3 A). *Sumf1*$^{-/-}$ HSPCs were cultured in the presence of UO126, and Western blotting was then performed on the protein homogenates. Phosphorylation of ERK was completely abolished in these UO126-treated cells, and GSK3-β phosphorylation was also blocked. Remarkably, β-catenin did not accumulate in these cells, and remained at levels comparable to WT HSPCs (Fig. 3 A, lanes 1–3).

In addition, we examined the accumulation of two transcription factors that regulate erythroid and myeloid differentiation: C/EBPα and GATA-1 (Laiosa et al., 2006b; Tsai et al., 1989). Semiquantitative PCR analysis and Western blotting showed that both C/EBPα and GATA-1 accumulate in *Sumf1*$^{-/-}$ HSPCs (Fig. S2 and Fig. 3 A, lane 2). Their levels were substantially diminished in UO126-treated *Sumf1*$^{-/-}$ HSPCs, and were comparable to those of WT HSPCs (Fig. 3 A, lanes 1–3). Thus, C/EBPα was up-regulated here by increased levels of p-ERK, as has been previously shown (Prusty et al., 2002). Interestingly, we

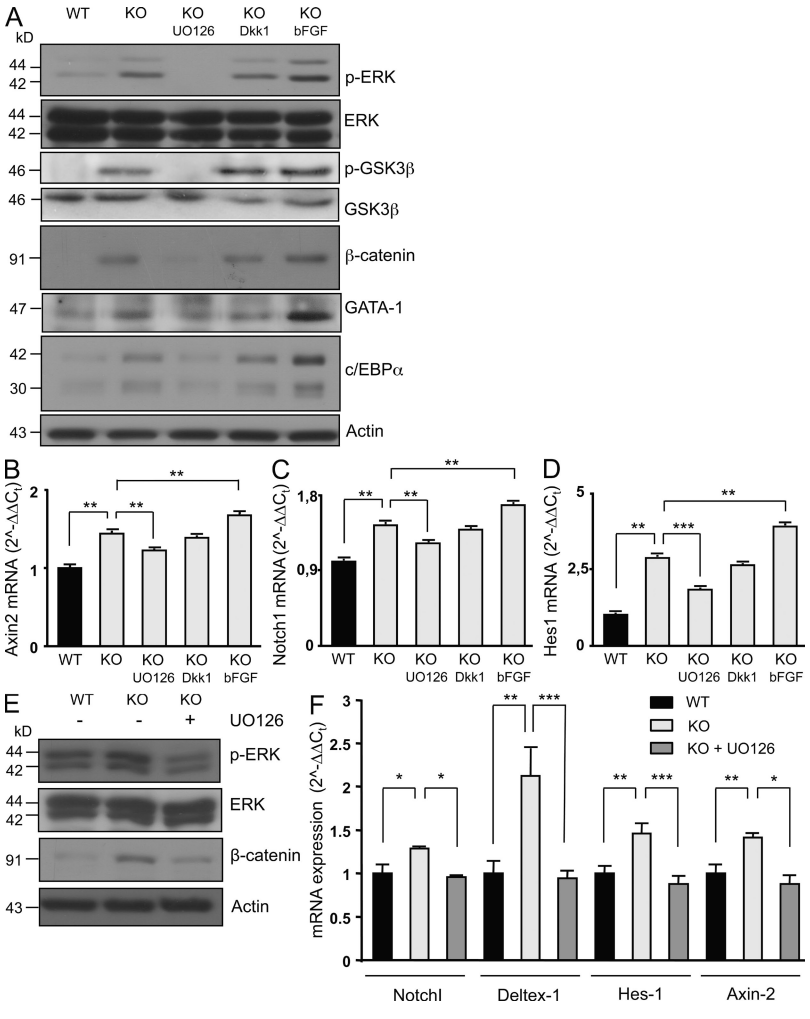

Figure 3. FGF-mediated activation of Wnt and Notch1 signaling pathways in HSPCs and MSCs from *Sumf1*$^{-/-}$ mice. (A) Western blot of total lysates from WT and *Sumf1*$^{-/-}$ (KO) HSPCs cultured without or with 100 μM UO126, 100 ng/ml Dkk1, or 100 ng/ml bFGF, as indicated. The loading controls were anti-actin, anti-ERK1/ERK2, and anti-GSK3β. The images are representative of four independent experiments (n = 4 for each group). (B–D) Quantitative RT-PCR analyses of *Axin-2* (B), *Notch1* (C), and *Hes1* (D) in WT and KO HSPCs grown under standard conditions or treated with UO126, Dkk1, and bFGF, as in A. Data are means ± SE (n = 3 for each group; *, P ≤ 0.05; **, P ≤ 0.01; ***, P ≤ 0.005). (E) Western blot of protein extracts from WT and KO MSCs cultured without or with 100 μM UO126. (F) Quantitative RT-PCR analysis of WT and KO MSCs, as in B–D, including *Deltex-1*. E and F are representative of two independent experiments (n = 4 for each group).

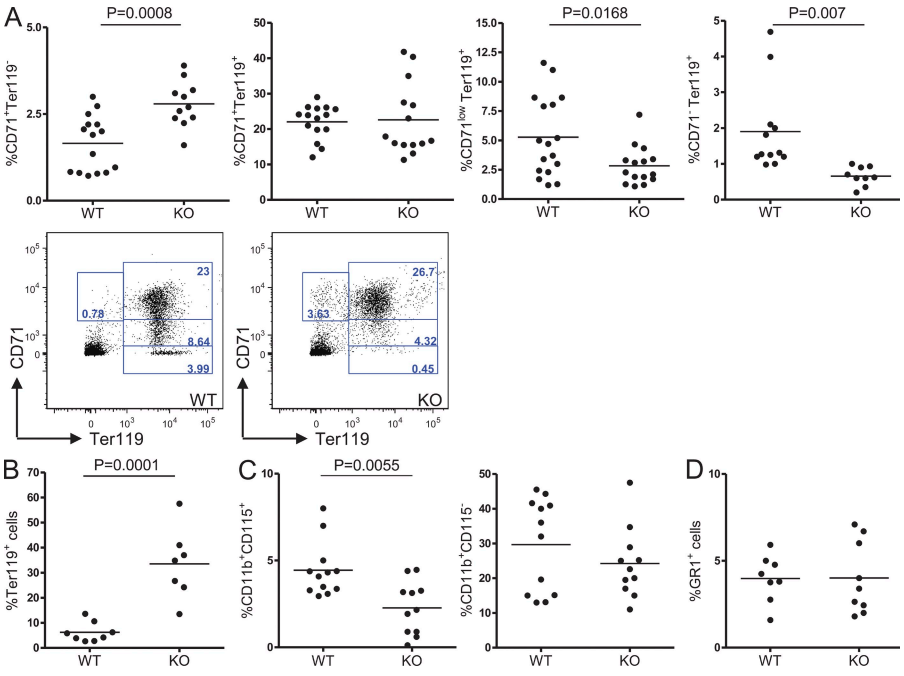

Figure 4. Erythroid and myeloid differentiation in *Sumf1*$^{-/-}$ mice. (A) Erythroid differentiation in BM of WT (n = 15) and *Sumf1*$^{-/-}$ (KO; n = 14) mice. Charts represent the percentages of marker +/− cells according to legend on Y axes; each dot represents one mouse, means are shown. Representative dot plots are shown below. Numbers in dot plots indicate percentage of cells in each gate. (B) The percentages of Ter119^{+} erythroid cells in the spleen of WT (n = 8) and KO (n = 7) mice. (C) Monocyte (CD11b^{+} CD115^{+}) and granulocyte (CD11b^{+} CD115^{-}) frequencies in the BM of WT (n = 13) and KO (n = 12) mice. (D) Granulocyte (Gr^{+}) frequency in the spleen of WT (n = 8) and KO (n = 9) mice. Unpaired Student's t test statistical analysis was performed, and P values are reported when significant. Each experiment was repeated four times.

also saw a marked p-ERK–dependent increase in GATA-1 levels. Conversely, there were similar levels of β-catenin, p-ERK, and c/EBPα in *Sumf1*$^{-/-}$ HSPCs that was not dependent on whether they were treated with Dkk1, a Wnt pathway inhibitor that acts on the Frizzled receptor (Bafico et al., 2001; Fig. 3 A, lanes 2 and 4). As expected, bFGF treatment of HSPCs increased p-ERK and p-GSK3-β even further, in respect to untreated *Sumf1*$^{-/-}$ cells; in turn, c/EBPα, GATA-1, and β-catenin accumulated accordingly (Fig. 3 A, lanes 2 and 5). In addition, *Axin2* and *Notch1*, which are β-catenin target genes, and *Hes-1*, a Notch1 target gene, were up-regulated in *Sumf1*$^{-/-}$ HSPCs, in respect to WT HSPCs. These levels were diminished by treating the cells with UO126, but not with Dkk1, whereas FGF treatment resulted in an increase in the expression levels in respect to the untreated *Sumf1*$^{-/-}$ HSPCs (Fig. 3, B–D). These data clearly show that SUMF1 inactivation results in an increase in ERK phosphorylation, which in turn leads to β-catenin, c/EBPα, and GATA-1 accumulation. *Sulf1/2*$^{-/-}$ double-KO mice also showed c/EBPα and GATA-1 accumulation (unpublished data).

HSCs are regulated by extrinsic cues, such as a variety of cytokines, growth factors, and ligands, and multiple developmental signaling pathways. The regulation of Wnt, BMP, Notch, Hedgehog, and FGF signaling pathways can contribute to the modulation of HSC-niche activity and can influence the quiescence state and mobilization of HSCs, and their recruitment to the vascular niche (Blank et al., 2008). Thus, we investigated the activation of the Wnt/β-catenin and FGF pathways in mesenchymal stromal cells (MSCs), which are nonhematopoietic cells that support HSC activities and functions in the niche. The MSCs isolated from the total BM of WT and *Sumf1*$^{-/-}$ littermates at 3 wk of age showed increased p-ERK, accumulation of β-catenin, and a consequent increased transcription of *Notch1, Deltex-1*, *Hes-1*, and *Axin2* (Fig. 3, E and F). Inhibition of ERK phosphorylation by UO126 in *Sumf1*$^{-/-}$ MSCs led to reduced accumulation of β-catenin and down-regulation of target genes (Fig. 3, E and F).

These data indicate that SUMF1 controls the FGF signaling pathway, which in turn also regulates the amount of β-catenin accumulation, also in the stromal component of the HSC niche.

SUMF1 loss of function results in a multilineage differentiation block

Next, we investigated whether altered Wnt and FGF signaling pathways and the accumulation of c/EBPα and GATA-1 transcription factors can result in differentiation impairment of HSCs in *Sumf1*$^{-/-}$ mice.

We first quantified the total number of cells in the BM, spleen, and thymus of *Sumf1*$^{-/-}$ mice, as compared with age-matched WT littermates, with organ cellularity adjusted according to body or organ weights (caused by the very low body weights of the mutant mice). There was low cellularity in the hematopoietic organs of *Sumf1*$^{-/-}$ mice, as compared with WT controls (Fig. S3, tables I and II). Similar differences in cellularity were also seen in the spleen and thymus of *Sulf2*$^{-/-}$ mice, although these were not seen in the *Sulf1*$^{-/-}$, *Ids*$^{-/-}$, and *Sgsh*$^{-/-}$ mice (Fig. S3, tables III and IV, and not depicted).

We then studied the phenotype of the BM of *Sumf1*$^{-/-}$ mice. A cohort of ≥14 *Sumf1*$^{-/-}$ mice and age- and sex-matched WT mice (4 wk old) were sacrificed, and their BM cells were flushed from their long bones and characterized by multichannel FACS analysis, for the expression of lineage/differentiation-stage markers.

Erythroid differentiation normally progresses from CD71^{+}Ter119$^{low/-}$ pro-erythroblasts through CD71^{+}Ter119^{+} basophilic erythroblasts, CD71^{low} Ter119^{+} chromatophilic

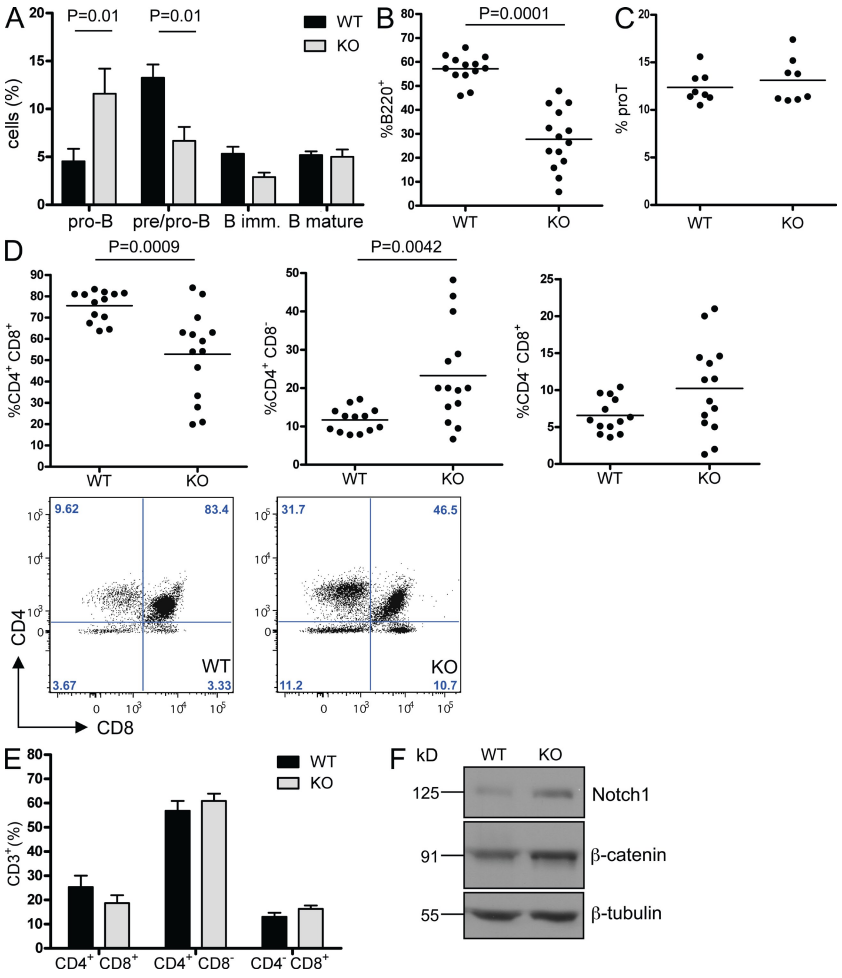

Figure 5. Lymphoid differentiation in *Sumf1*$^{-/-}$ mice. (A and B) Differentiation of B cells in BM (A) and spleen (B) of WT (n = 13) and *Sumf1*$^{-/-}$ (KO; n = 14) mice. (A) Different stages of B cell maturation were defined according to expression of IgM, B220, and CD127 markers (mean ± SD). (B) B220^{+} cells in spleen of WT (n = 13) and KO (n = 14) mice. (C–E) Differentiation of T cells in BM (C) and thymus (D and E) of WT (n = 13) and KO (n = 14) mice. (C) Percentages of pro–T cells (CD127^{+} CD3^{-} CD4^{-} CD8$^{-/low}$ CD25^{-} c-kit^{+}) in BM. (D) Percentages of thymocytes in indicated subsets (representative plots are shown below graphs). Each dot represents one mouse, means are shown. (E) Percentage of cells in indicated subsets gated on CD3^{+} thymocytes. Unpaired Student's t test statistical analysis was performed, and p-values are reported when significant. (F) Western blots of total homogenates from WT (n = 6) and KO (n = 6) HSPCs with the indicated antibodies. Data are representative of six independent experiments.

erythroblasts, and CD71^{-}Ter119$^{+/high}$ orthochrotomaphilic erythroblasts. In the *Sumf1*$^{-/-}$ BM, we saw accumulation of CD71^{+}Ter119$^{low/-}$ pro-erythroblasts and a strong reduction in CD71^{low} Ter119^{+} chromatophilic erythroblasts and mature CD71^{-}Ter119^{high} orthochrotomaphilic erythroblasts, indicating a block in erythroid differentiation (Fig. 4 A). The accumulation of erythroblasts in the spleen of *Sumf1*$^{-/-}$ mice might reflect a compensatory response to ineffective erythropoiesis, or a peripheral accumulation of immature cells (Fig. 4 B). An increase in CD71^{+}Ter119$^{low/-}$ pro-erythroblasts was also seen in *Sulf2*$^{-/-}$ mice, but not in *Sulf1*$^{-/-}$, *Ids*$^{-/-}$, or *Sgsh*$^{-/-}$ mice (Fig. S4, A and B, and not depicted). No differences were detected in the percentages of BM CD71^{low}Ter119^{+}, of BM CD71^{-}Ter119^{high}, and of spleen Ter119^{+} cells from these animal models (Fig. S4 C). In the BM of *Sumf1*$^{-/-}$ mice, there was also a marked reduction in monocytes (CD11b^{+} and CD115^{+}) and a slight decrease in granulocytes (CD11b^{+} and CD115^{-}), as compared with WT mice, with no differences in their percentages in the spleen (Gr-1^{+}; Fig. 4, C and D). In contrast, myeloid development progressed normally in the *Sulf1*$^{-/-}$, *Sulf2*$^{-/-}$, *ids*$^{-/-}$, and *sgsh*$^{-/-}$ mice (unpublished data).

Overall, these data indicate that SUMF1 contributes to the regulation of the development of the erythroid and myeloid lineages, and that SUMF1 loss of function results in a significant loss of erythroid and myeloid terminally differentiated cells.

B lymphocytes differentiate in the BM from a common lymphoid progenitor (CLP) through a series of well-defined intermediates. We analyzed the pro–B cell stage (CD127^{+}, B220^{low}, IgM^{-}) in the BM of *Sumf1*$^{-/-}$ mice, in comparison with WT littermates: there was an accumulation of pro–B cells, a reduction in immature B cells (CD127^{-}, B220^{low}, IgM^{+}), and apparently normal percentages of mature B cells (B220^{high}, IgM^{+}; Fig. 5 A). However, a strong decrease in terminally differentiated B lymphocytes (B220^{+}) was seen in the spleen of mutant mice (Fig. 5 B). These data led us to conclude that there was a block in maturation of B lymphocytes at the pro–B stage. Absolute B cell counts in the spleen confirmed this finding (unpublished data), thus weakening the alternative hypothesis, that lack of terminally differentiated B cells is a secondary effect caused by the erythroid expansion occurring in the spleen of the *Sumf1*$^{-/-}$ mice. No differences were detectable in pro–B and mature B cells in any of the other mice models analyzed, with the exception of *Sulf2*$^{-/-}$ mice, in which a slight decrease in immature and mature B lymphocytes was seen in the BM, although this was in the absence of a defect in mature cells in the spleen. (Fig. S5, A and B).

Next, we analyzed T cell development. As with B lymphocytes, T cells originate from a CLP, but during differentiation, the pro–T cell (c-kit^{+}, CD127^{+}, CD25^{-}, CD3^{-}, CD4^{-}, and CD8^{-}) BM-resident cells migrate into the thymus to give rise to mature T lymphocytes. *Sumf1*$^{-/-}$ and WT mice had similar pro–T cell percentages in the BM (Fig. 5 C). However, a reduction in immature double-positive (DP) CD4^{+} CD8^{+} thymocytes and an increase in single-positive (SP) CD4^{+} or SP CD8^{+} thymocytes were seen in the thymus of *Sumf1*$^{-/-}$ mice (Fig. 5 D). The CD4 and CD8

antigens are expressed only after CD3 (a TCR accessory protein; Clevers et al., 1988; Teh et al., 1988). By looking at the $CD3^+$ population, no differences in the frequencies of SP $CD3^+$ $CD4^+$ and SP $CD3^+$ $CD8^+$ cells were seen in *Sumf1*$^{-/-}$ mice, as compared with WT mice, clearly showing the existence of aberrant *Sumf1*$^{-/-}$ populations of $CD4^+$ and $CD8^+$ thymocytes that did not express CD3 (Fig. 5 E). This might be caused by accumulation of *Notch1* and β-catenin in the *Sumf1*$^{-/-}$ thymocytes (Fig. 5 F). Indeed, *Notch1* has been shown to substitute for CD3 expression in promoting development of thymocytes from the DP to SP stages (Deftos et al., 2000; Michie et al., 2007). In the *Sulf1*$^{-/-}$, *Ids*$^{-/-}$, and *Sgsh*$^{-/-}$ mice, pro–T cells, total DP and SP thymocytes, and DP and SP cells gated on $CD3^+$ were comparable in frequency to those of WT mice (Fig. S5, C–H, and not depicted). However, a slight decrease in DP thymocytes and a parallel increase in SP $CD4^+$ cells was seen in *Sulf2*$^{-/-}$ mice when gated both on the total population and on the $CD3^+$ cells (Fig. S5, F–H). Interestingly, development of invariant natural killer T cells, a highly specialized subset of thymocytes, was also severly impaired in the *Sumf1*$^{-/-}$ mice (Plati et al., 2009).

The stem/early progenitor cell compartment is not affected in bone marrow of *Sumf1*$^{-/-}$ mice

The HSC-enriched KLS compartment, defined as c-kit^+, Lin^-, $Sca1^+$, includes LT-HSCs, ST-HSCs, and multipotent progenitor (MPP) cells (Spangrude et al., 1988; Laiosa et al., 2006a). The analysis of the lineage-negative HSPC population of WT and *Sumf1*$^{-/-}$ mice revealed a similar content of KLS cells in the BM (Fig. 6 A). In addition, to identify LT-HSCs (c-kit^+, Lin^-, $Sca1^+$, and $CD150^+$), ST-HSCs, and MPP cells (ST-HSC/MPP: c-kit^+, Lin^-, $Sca1^+$, and $CD150^-$), we analyzed the CD150 marker in KLS cells. Comparable proportions of LT-HSCs and ST-HSC/MPP cells were present in the BM of *Sumf1*$^{-/-}$ and WT mice (Fig. 6 B).

The HSPC fraction also includes early committed progenitor cells, such as CLPs and common myeloid progenitors (CMPs). The CLP population differentiates subsequently into pro–T and pro–B cells, whereas the CMP population generates megakaryocyte–erythrocyte progenitors (MEPs) and granulocyte–monocyte progenitors (GMPs; Morrison and Weissman, 1994; Morrison et al., 1995; Kondo et al., 1997; Akashi et al., 2000; Laiosa et al., 2006a). To evaluate the relative frequencies of these progenitor cells, *Sumf1*$^{-/-}$ and WT HSPCs were stained for $Sca1^+$, c-kit^+, CD127, CD16, and CD34. Flow cytometry analysis revealed no significant differences in the contents of CMPs (Lin^-, c-kit^+, $Sca1^-$, $CD127^-$, $CD34^{high}$, and $CD16^{low}$), MEPs (Lin^-, c-kit^+, $Sca1^-$, $CD127^-$, $CD34^-$, and $CD16^{low}$), GMPs (Lin^-, c-kit^+, $Sca1^-$, $CD127^-$, $CD34^{high}$, and $CD16^{high}$), and CLPs (Lin^-, c-kit^+, $Sca1^+$, and $CD127^+$) in *Sumf1*$^{-/-}$ HSPCs, in respect to WT cells; however, the progenitor cells showed a tendency to increase in *Sumf1*$^{-/-}$ HSPCs, in respect to the WT cells (Fig. 6 C). No major differences in HSPC subfractions were seen in *Ids*$^{-/-}$, *Sulf1*$^{-/-}$, and *Sulf2*$^{-/-}$ mice (unpublished data).

In vivo inhibition of the FGF pathway overcomes the SUMF1-dependent multilineage differentiation block

To further demonstrate that the constitutive FGF signaling that leads to β-catenin accumulation is responsible for the multilineage differentiation block seen in *Sumf1*$^{-/-}$ mice (Figs. 4 and 5), we wanted to unlock the differentiation of *Sumf1*$^{-/-}$ terminal lineages by inhibiting FGF1 signaling in vivo with SU5402, a specific FGF1 receptor antagonist. Thus, *Sumf1*$^{-/-}$ mice were i.p. injected at postnatal day (P) 7 with a suspension of 500 μM SU5402 adsorbed onto beads (to allow slow SU5402 release). The mice were then analyzed at P21–P27 (Fig. 7 A). Upon SU5402 treatment, the frequency of intermediate precursors and terminally differentiated $CD71^-Ter119^+$ cells significantly increased in the BM of *Sumf1*$^{-/-}$ mice, demonstrating a rescue of the block of erythroid lineage differentiation (Fig. 7 B). Similarly, the myeloid lineage was unlocked, and comparable frequencies of monocytes and granulocytes were seen, in respect to those in the BM of WT littermates (Fig. 7 C). Moreover, SU5402 also increased the mature B lymphocytes

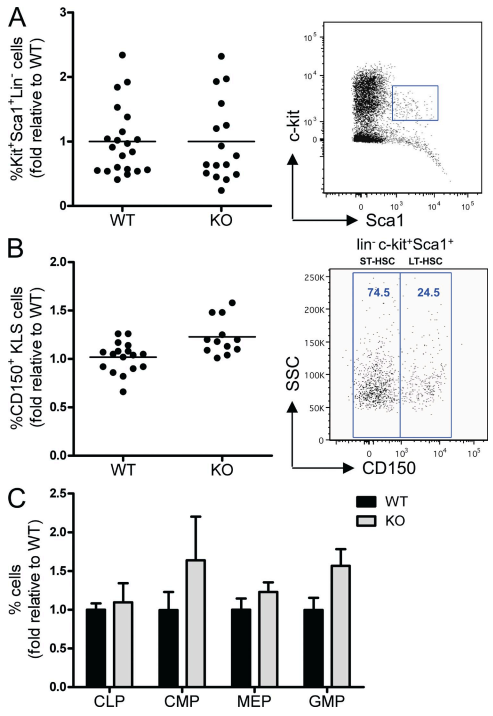

Figure 6. Characterization of HSC and progenitor subsets. Percentage of $Sca1^+$ c-kit^+ HSCs (A) and LT-HSCs ($CD150^+$; B) in lineage-negative BM of WT ($n = 21$) and *Sumf1*$^{-/-}$ (KO; $n = 16$) mice (each dot represents 1 mouse; results are expressed as fold relative to WT). Representative plots are shown on the right. (C) Percentage of CLPs, common myeloid progenitors (CMPs), megakaryocyte-erythrocyte progenitors (MEPs), and granulocyte-monocyte progenitors (GMPs) in BM of KO mice expressed as fold to WT mean (means ± SD; $n = 6$). Unpaired Student's *t* test (A and C) or Mann-Whitney (B) statistical analysis were performed, and p-values are reported when significant. Each experiment was repeated three times.

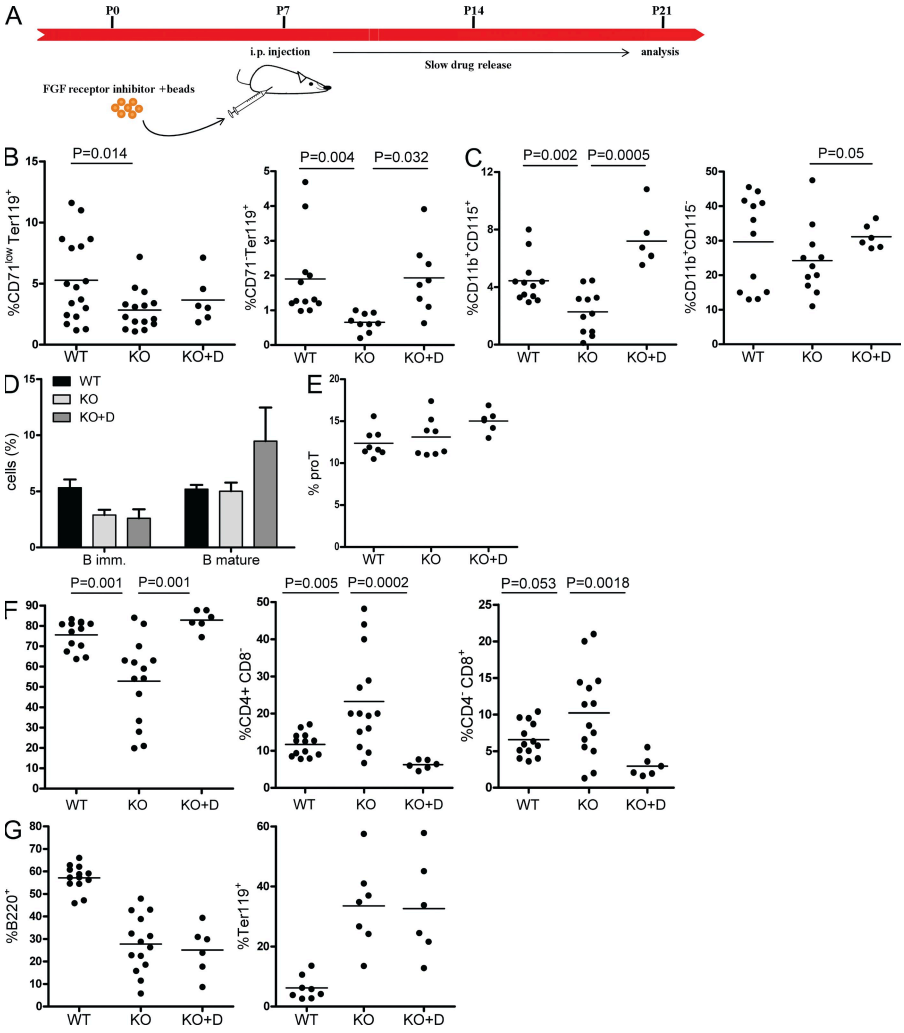

Figure 7. SU5402-FGFR blocker reverted the terminal multilineage differentiation blocks in *Sumf1*$^{-/-}$ mice. (A) Experimental timeline. *Sumf1*$^{-/-}$ mice were i.p. injected at P7 with a suspension of FGFR inhibitor adsorbed on beads. The animals were then sacrified at P21-P27 and BM, spleen and thymus phenotype analysis were performed. (B) Erythroid differentiation in BM of WT ($n = 17$), *Sumf1*$^{-/-}$ (KO; $n = 15$) and *Sumf1*$^{-/-}$ KO treated ($n = 6$; KO+D) mice. Charts represent the percentages of cells in each subset; each dot represents one mouse, means are shown. (C) Monocyte and granulocyte frequencies in the WT ($n = 12$), KO ($n = 11$) and KO-treated ($n = 6$) mice. (D) B cell maturation in WT ($n = 7$), KO ($n = 9$), and KO-treated mice ($n = 6$), according to expression of IgM, B220, and CD127 markers. (E and F) Differentiation of T cells in BM (E) and thymus (F) of WT ($n = 13$) and KO ($n = 14$) and KO-treated ($n = 6$) mice. (E) Percentages of pro-T cells in BM of WT ($n = 8$), KO ($n = 8$) and KO+D ($n = 6$). (F) Percentages of thymocytes in each subset (WT, $n = 13$; KO, $n = 14$; drug-treated KO, $n = 6$). (G) B lymphocytes (B220$^+$) and erythrocytes (Ter-119$^+$) in the spleen of WT ($n = 13$), KO ($n = 14$), and treated KO ($n = 6$) mice. Unpaired *t* test statistical analysis was performed, and P values are reported when significant. Analysis of two independent experiments.

in treated mutants, as compared with untreated mice (Fig. 7 D). Although SU5402 treatment did not affect the pro–T frequency in the BM (Fig. 7 E), thymocytes developed normally; comparable DP and SP T lympocyte frequencies were seen in the treated mutants, both for the total (Fig. 7 F) and for electronically gated CD3$^+$ populations (not depicted), in respect to WT mice. We did not observe any correction/restoration of the erythrocyte and B lymphocyte proportions in the spleen of treated mice, which was probably because we analyzed the mice 2–3 wk after SU5402 administration, a time that is too early to see any rescue effect (Fig. 7 G).

Collectively, these findings demonstrate that SUMF1 controls hematopoietic lineage differentiation via modulation of the FGF pathway.

Sumf1$^{-/-}$ HSPCs fail to differentiate in a wild-type host, and transplanted mice show the *Sumf1*$^{-/-}$ hematopoietic phenotype

To demonstrate that differentiation defects of *Sumf1*$^{-/-}$ HSPCs are cell autonomous and independent of the cell niche, we transplanted these into WT recipient mice. Purified WT HSPCs and *Sumf1*$^{-/-}$ HSPCs were transduced with a LV vector carrying GFP cDNA, to follow their long-term fate after transplantation (Biffi et al., 2004). LV-transduced HSPCs (7×10^5) were transplanted into lethally irradiated, 2-mo-old WT recipient mice. 10 wk after noncompetitive transplantation, the hematopoietic organs were collected and analyzed by flow cytometry, as described above. The cells of donor origin were analyzed according to GFP expression. This analysis showed a considerable reduction in the total cell number in the BM, spleen, and thymus of mice transplanted with *Sumf1*$^{-/-}$ HSPCs, with respect to mice transplanted with WT cells (Fig. 8 A), as also seen in the donor mice. Interestingly, the overall engraftment of GFP$^+$ *Sumf1*$^{-/-}$ and WT HSPCs were comparable (Fig. 8 B). All further analyses were performed on the GFP$^+$ population to avoid confounding effects from residual autologous cells. When we analyzed terminally differentiated cells in the BM, spleen, and thymus of the transplanted mice, a block in erythroid lineage differentiation of the *Sumf1*$^{-/-}$ HSPCs transplanted mice was clearly seen, as strong reductions in the frequencies of CD71^{low}Ter119$^+$ chromatophilic erythroblasts and of mature CD71$^-$Ter119^{high} orthochrotomaphilic erythroblasts (Fig. 8 C). Notably, and probably because of the limited time of observation (10 wk after the transplant), in these mice we did not detect any accumulation of CD71$^+$Ter119$^+$ cells in the BM, although the same

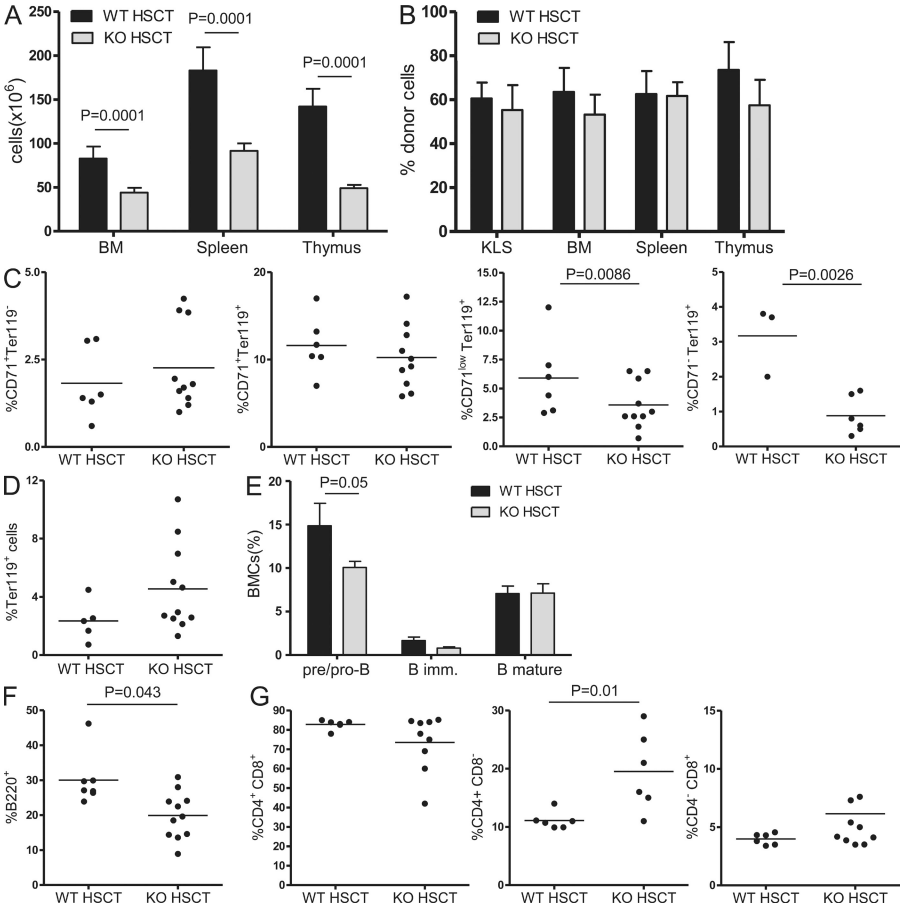

Figure 8. *Sumf1*$^{-/-}$ HSPC differentiation in wild-type hosts. (A) Total cell count of BM, spleen, and thymus of mice transplanted with WT (WT HSCT, $n = 8$) or *Sumf1*$^{-/-}$ HSPCs transduced with GFP-expressing LV (KO HSCT, $n = 11$; means ± SD). (B) Engraftment of GFP$^+$ HSCs in the KLS fraction (Sca1$^+$ c-kit$^+$ HSCs from lineage-negative selected BM) or in total BM, spleen, and thymus of WT HSCT and KO HSCT mice (means ± SD). (C) Erythroid differentiation in BM and spleen (D) of WT HSCT and KO HSCT mice. (E) Different stages of B cell maturation were defined according to expression of IgM, B220, and CD127 markers (means ± SD). (F and G) Percentage of lymphoid B220$^+$ cells in spleen (F) and (G) percentage of thymocyte subsets in WT HSCT and KO HSCT mice. Charts: each dot represents one mouse, means are shown. Unpaired Student's *t* test statistical analysis was performed, and p-values are reported when significant. The transplantation experiment was performed two times.

compensatory increase in Ter119$^+$ cells was seen in the spleens of the donors (Fig. 8 D).

Impaired B cell development and aberrant T cell development were seen in the *Sumf1*$^{-/-}$ HSPCs transplanted mice, which showed a decrease in pre–/pro–B cells, low percentages of terminally differentiated B cells in the spleen, a reduction in DP CD4$^+$ CD8$^+$ cells in the thymus, and an increase in SP CD4$^+$ and SP CD8$^+$ thymocytes (Fig. 8, E–G). In addition, as for the donor mice, there was aberrant CD3$^-$ SP CD4$^+$ and SP CD8$^+$, without expression of the TCR accessory protein (unpublished data).

Furthermore, although the number of granulocytes and monocytes in the BM were similar in both of these groups of transplanted mice, there was a slight decrease in Gr-1$^+$ cells in the spleen of the *Sumf1*$^{-/-}$ HSPCs transplanted mice, leading us to envision a compensatory mechanism in the BM, with mutated cells that might unlock GMP progression into differentiation (unpublished data).

Finally, we analyzed the HSPC fraction in both of these groups of transplanted mice. Interestingly, there was a slight increase (although not statistically significant) in the frequency of KLS cells in the mice transplanted with *Sumf1*$^{-/-}$ GFP$^+$ HSPCs (Fig. 9 A). Within the KLS cells, we saw a decrease in the frequency of CD150$^+$ LT-HSCs and a consequent increase in the ST-HSC/MPP fraction in the group of *Sumf1*$^{-/-}$ HSPC transplanted mice (Fig. 9 B), suggesting that the SUMF1 defect might render primitive HSC more prone to differentiate into ST-HSCs and MPPs. Furthermore, there were relevant increases in CLPs and CMPs in the *Sumf1*$^{-/-}$ HSPC transplanted mice (although, not statistically significant; Fig. 9 C).

In conclusion, transplantation of *Sumf1*$^{-/-}$ HSPCs reproduces the phenotype of *Sumf1*$^{-/-}$ mice in a WT host,

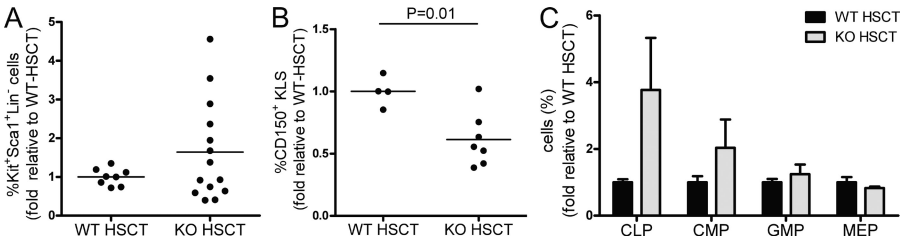

Figure 9. HSC and progenitor characterization in recipients of GFP-expressing *Sumf1*$^{-/-}$ HSPCs. (A) GFP$^+$ Sca1$^+$ c-kit$^+$ HSCs in lineage-negative selected BM of recipient of WT ($n = 8$) and KO ($n = 11$) HSCT (WT-HSCT and KO-HSCT mice). Each dot represents one mouse. Mean ± SD are shown; mean of two independent experiments. (B) LT-HSCs (GFP$^+$ CD150$^+$ KLS) from WT-HSCT and KO-HSCT (each dot represents a pool of two mice). (C) CLPs, CMPs, MEPs, and GMPs in BM of WT and KO HSCT mice expressed as fold to WT average. (means ± SD; $n = 6$; analysis of two independent experiments). Mann-Whitney test statistical analysis was performed, and p-values are reported when significant.

leading us to conclude that SUMF1 has an important role in different steps of the lineage differentiation process of HSPCs.

DISCUSSION

HSCs represent a rare population of adult stem cells that can give rise to all blood cell lineages in a hierarchical process that occurs daily in adult mammals (Morrison and Weissman, 1994; Morrison et al., 1995; Kondo et al., 1997; Akashi et al., 2000; Laiosa et al., 2006a). The more the cells proceed in the developmental progression, the more restricted they become in their differentiation potential, losing their self-renewal ability. Cytokines, hormones, and activation of different signaling pathways control these well-tuned developmental processes that couple and integrate extrinsic and intrinsic fate determinants. Developmentally conserved signaling pathways have emerged as important controlling devices for HSC fate, including Wnt, FGF, Notch, sonic hedgehog (Shh), and bone morphogenetic protein (BMP; Esko and Lindahl, 2001).

Several studies have reported on the role of the Wnt/β-catenin pathway in controlling self-renewal and differentiation of HSCs in vivo and ex vivo, with apparent discrepancies seen. Some studies claim that stabilization of β-catenin is positive for self-renewal and differentiation of HSCs (Reya et al., 2003; Willert et al., 2003; Baba et al., 2005), whereas others assert that β-catenin stabilization impairs HSC repopulation and engraftment in a recipient (Kirstetter et al., 2006; Scheller et al., 2006). We believe that fixed β-catenin thresholds at specific developmental stages can provide different phenotypes. This is evident in different biological contexts, such as during cardiac differentiation: differentiating embryonic stem cells treated early with Wnt-3a undergo cardiac differentiation; conversely, late activation of the Wnt pathway reduces their cardiac differentiation (Ueno et al., 2007). Periodic β-catenin accumulation in embryonic stem cells at a specific threshold can lead to reprogramming of somatic cells after fusion. In contrast, high or low levels of β-catenin can affect the ability of embryonic stem cells to reprogram somatic cells (Lluis et al., 2008).

This scenario is even further complicated, as many signaling pathways show cross-talk, and their interactions will determine the different developmental fates in blood lineages. An interaction between the Shh and BMP-4 pathways is evident in the finding that Shh can induce proliferation of primitive hematopoietic cells via BMP-4 (Bhardwaj et al., 2001). However, BMP-4 can maintain HSCs *in culture*, but cannot control their expansion (Utsugisawa et al., 2006). FGFs and Wnts have also been shown to interact in a variety of developmental systems, including brain, kidney, and tooth in some vertebrates (Moon et al., 1997), and FGF signaling controls proliferation and subsequent lineage commitment of neural stem cells through a concerted action with β-catenin (Israsena et al., 2004). The role of the FGF signaling pathway in the development of blood lineages is poorly understood, with FGF1 and FGF2 used for ex vivo culture of LT-HSCs, together with some additional growth factors and cytokines (Yeoh et al., 2006). In contrast, TGF-β is generally accepted to be a potent inhibitor of HSC expansion in vitro (Sitnicka et al., 1996; Batard et al., 2000).

So, overall, very little is known about the cross-talk between these signaling pathways. It is certain that the influences they have on each other will finally regulate the complex hierarchical development of different blood lineages. If one signaling pathway is imbalanced or dysregulated, it might lead to cells of one lineage being reprogrammed into another lineage, thus resulting in a change in cell fate. This can arise from aberrant expression of key transcription factors, such as GATA-1, GATA-3, C/EBPα, and PU.1 (Orkin and Zon, 2008). Indeed, it has been shown that myeloid transdifferentiation of pro–B cells is caused by ectopic expression of c/EBPα (Heavey et al., 2003). This might also account for the compensation of the granulocytes that we see in the *Sumf1*$^{-/-}$ mice.

Here, we have shown direct interconnections between at least three different pathways: FGF, Wnt/β-catenin, and Notch signaling. These are regulated by the activity of SUMF1, probably via the Sulf1 and Sulf2 sulfatases. We have shown that activation of the FGF signaling pathway leads to increases in ERK phosphorylation that, upon GSK-3 inactivation, trigger β-catenin accumulation. In thymocytes, we observed FGF-dependent accumulation of β-catenin and Notch activation. Interestingly, SUMF1 controls autophagy, proliferation, and differentiation of chondrocytes by limiting FGF signaling (Settembre et al., 2008). The constitutive activation of FGF and Wnt/β-catenin leads to an increase in ST-HSCs, as clearly seen in the recipient transplanted mice. As a result, a lack of terminally differentiated cells occurs because of developmental failure in the three lineages; in addition, aberrant thymocytes also develop. The concerted activities of accumulated β-catenin and *Notch1* might, in part, stall the transition of thymocytes from the double-negative to the DP stage, and increase the levels of SP CD4$^+$ or CD8$^+$ thymocytes; indeed, it has been shown that β-catenin can, in part, transcribe the *CD4* gene (Huang et al., 2006) and increase the timing and maturation rate of CD8$^+$ cells (Yu and Sen, 2007; Staal and Sen, 2008). The rescue of erythroid lineage differentiation and the normal development of T lymphocytes after FGF1 signaling inhibition in *Sumf1*$^{-/-}$ mice further reinforce the observation that FGF activation controls Wnt and Notch signaling activation in the differentiation of HSPCs.

In the *Sulf2*$^{-/-}$ mice, there was a slight increase in proerythroblasts, a small decrease in BM B mature cells, a decrease in DP thymocytes, and an increase in SP CD4$^+$ cells, and we would expect lineage defects to be even more severe in the *Sulf1*$^{-/-}$ *Sulf2*$^{-/-}$ double-KO mice because of the redundancy in the activities of these two sulfatases (Ratzka et al., 2008). This double-KO phenotype is very severe and the mice die very early (Holst et al., 2007); indeed, we only obtained a sufficient number of these *Sulf1*$^{-/-}$ *Sulf2*$^{-/-}$ double-KO mice for the biochemical analysis here. Sulf1$^{-/-}$

Sulf2$^{-/-}$ HSPCs showed constitutive activation of FGF and Wnt signalings. Unfortunately, because of the severe phenotype and the lack of *Sulf1*$^{-/-}$ *Sulf2*$^{-/-}$ double-KO mice, we could not carry out the BM phenotype analysis. In contrast, *Ids*$^{-/-}$ and *Sgsh*$^{-/-}$ mice did not show any of the defects seen in the *Sumf1*$^{-/-}$ strain, ruling out any involvement of these other sulfatases in the hematopoietic lineage phenotype.

Mesenchymal stromal cells (MSCs) reside in the niche that supports stem cell activity in vivo. MSCs from *Sumf1*$^{-/-}$ mice show constitutive activation of the FGF and Wnt signaling pathways. These might induce irreversible conditioned functions in the HSCs. Osteoblasts overexpressing the Wnt inhibitor Dkk1 have irreversible effects on HSC function, reducing their ability for long-term repopulation in serial transplant experiments (Fleming et al., 2008). It is possible that concerted dysregulation of the FGF, Wnt/β-catenin, and Notch signaling pathways in both the MSC niche component and in the HSCs themselves forces the HSC pool to enter into the cell cycle, and thus to switch them toward a short-term reconstituting phenotype, with a consequent decrease in terminally mature cell development.

Moreover, we have also show that these altered interacting signaling pathways induce lineage defects in a mouse model of MSD. Patients affected by MSD show a lack of activity of their entire family of sulfatases, and the consequent accumulation of undegraded sulfatase substrates in their lysosomes. In addition, these patients have developmental problems that can be ascribed to a lack of activity of Sulf1 and Sulf2, the only sulfatases that can modulate signaling pathways. The lysosomal storage in murine models of sulfatase deficiencies does not cause defects in lineage development. In further support of these data, we recently showed that invariant natural killer T cells develop aberrantly only in the MSD mouse model, and not in lysosomal disease models (Plati et al., 2009), ruling out a role for lysosomal engulfment in lineage development.

Sulf1$^{-/-}$ *Sulf2*$^{-/-}$ double-KO mice and *Sumf1*$^{-/-}$ mice show very high perinatal mortality (Holst et al., 2007), and our data lead us to believe that blood lineage failure might contribute to this mortality. Alternatively, the MSD disease is very heterogeneous with respect to the developmental features, which is possibly caused by the escape of β-catenin stabilization in patients carrying less-detrimental *SUMF1* mutations. Interestingly, we observed that even in mixed background strains, the BM phenotype of *Sumf1*$^{-/-}$ mice is relatively heterogeneous, with some mice showing less severe defects (unpublished data).

All in all, our data highlight that regulation through the sulfation state of the HSPGs, which provide a repository of growth factors such as Wnt and FGF, should be finely tuned. This is also modulated by the Sulf activities (Dhoot et al., 2001; Ai et al., 2003; Viviano et al., 2004; Wang et al., 2004). Thus, we hypothesize that only a small fraction of Sulf proteins have the FGly residue and can cleave the sulfate of the heparan sulfate in HSPGs; the majority of the Sulfs should be activated by SUMF1. This represents a fine regulation mechanism, and SUMF1 appears to be the master controlling factor here.

MATERIALS AND METHODS

Mice. The strains used in this study were as follows: *Sumf1*$^{-/-}$ (Settembre et al., 2007), *Sulf1*$^{-/-}$, *Sulf2*$^{-/-}$ (Ai et al., 2003), *Ids*$^{-/-}$ (Cardone et al., 2006), and *Sgsh*$^{-/-}$ (Fraldi et al., 2007). All the procedures were approved by the Animal care and use Committee of Telethon Institute of Genetics and Medicine and were communicated to the Ministry of Health and local authorities, according to Italian law.

Flow cytometry analysis. A FACSCanto instrument (BD) was used for the FACS analysis. Phycoerythrin-conjugated anti–mouse mAbs to c-kit, CD34, CD71, CD3, CD4, IgM, and Gr-1; allophycocyanin-conjugated anti–mouse mAbs to Ter119, CD11b, CD16, CD25, and CD8; and phycoerythrin-conjugated-cycrome5 anti–mouse mAbs to B220, CD3, and 7-amino-actinomycin D were purchased from BD. Phycoerythrin-conjugated-cycrome7 anti–mouse mAbs to Sca1 and c-kit; allophycocyanin-conjugated-Alexa Fluor 750 anti–mouse mAbs to c-kit and CD8; and allophycocyanin-conjugated CD150 were purchased from eBioscience. The FITC-conjugated anti–mouse mAb to CD127 was purchased from Abcam, and the phycoerythrin-conjugated anti–mouse mAb to CD115 was purchased from Serotec. Isolated BM, spleen, and thymic cells were prepared for flow cytometry by blocking the aspecific sites using anti-Fc blocking reagent from BD, and then incubating the cells with the appropriate antibodies or control isotype-matched antibodies, followed by PBS washes.

HSPC transplantation. 2-mo-old C57Bl6 mice were lethally irradiated for 4 h before transplantation (10 Gy, divided into two doses). Next, 7×10^5 WT or *Sumf1*$^{-/-}$-transduced HSPCs were injected into the tail veins of the recipient mice. The transplanted mice were sacrificed 10 wk after transplantation, and their BM, spleen, and thymus were analyzed.

Statistics. Analyses were performed by one-way and two-way ANOVA, using Bonferroni correction as post-test, or Student's *t* test/Mann Whitney tests, and the data are expressed as means ± SD; p-values < 0.05 were considered statistically significant.

Purification and culture of mouse HSPCs. Total BM was flushed out from femurs and tibia of 3-wk-old and age-matched WT and *Sumf1*$^{-/-}$ mice. For in vitro experiments, the lineage-fraction was purified from total BM cells by untouched isolation on a magnetic sorter, using the Lineage Depletion kit (Miltenyi Biotec), according to the manufacturer protocol. The HSPCs were cultured for two days in Stem Span Sfem medium (STEMCELL Technologies) at a concentration of 10^6 cells/ml in the presence of 100 ng/ml recombinant mouse SCF (R&D Systems), 20 ng/ml mouse IL3 (Peprotech), 20 ng/ml human IL6 (Peprotech), and 10 ng/ml Flt3 ligand (Peprotech). They were then harvested for all of the analyses. HSPCs for the in vivo studies were purified from total BM cells by untouched isolation using the Murine Progenitor Enrichment Cocktail (STEMCELL Technologies).

Purification and culture of mouse mesenchymal stromal cells. Total BM was flushed out from femurs and tibia of 3-wk-old and age-matched WT and *Sumf1*$^{-/-}$ mice. The total cells were cultured for 3 d in DME with 10% FBS. The medium was then changed to remove nonadherent cells. The mesenchymal stromal cells (MSCs) were grown until confluence, and then harvested for analysis.

Splenocyte and thymocyte isolation. Splenocytes were obtained by mechanic disaggregation of the spleen in RPMI with 10% FBS, 100 IU/ml penicillin, 100 μg/ml streptomycin, 2 mM L-glutamine, supplemented with 28.4 mM 2-mercaptoethanol. The thymocytes were obtained by mechanic disaggregation of the thymus in IMDM with 20% FBS, 100 IU/ml penicillin, 100 μg/ml streptomycin, and 2 mM L-glutamine. After centrifugation at 1,500 rpm for 5 min at room temperature, 2.5×10^3 cells were resuspended in 50 μl blocking solution.

HSPCs transduction. Freshly isolated HSPCs from WT and *Sumf1*$^{-/-}$ mice were transduced with PGK.GFP.LV or 4xTCF/LEF.mCMV.eGFP or 4xERK.mCMV.eGFP, at a multiplicity of infection (MOI) of 100 in Stem Span Sfem medium (Stem Cell Technologies), at a concentration of 10^6 cells/ml in the presence of 100 ng/ml recombinant mouse SCF (R&D Systems), 20 ng/ml mouse IL-3 (Peprotech), 20 ng/ml human IL-6 (Peprotech), and 10 ng/ml Flt3 ligand (Peprotech) for 12–16 h. The transduction efficiency was evaluated at the clonal level on colonies from the colony-forming cell assay or by FACS analysis.

mSulf1/mSulf2 enzymatic activity assay. Total homogenates from WT and *Sumf1*$^{-/-}$ HSPCs were obtained using SIE buffer (250 mM saccharose, 3 mM imidazole, pH 7.4, 1% ethanol, and 1% NP-40). 10 µg total cell homogenates were incubated with 10 µM estrone 3-O-sulfamate at 37°C for 1 h, to inhibit steroid sulfatases, before addition of 10 mM 4-MUS substrate in 10 mM lead acetate buffer, for a total of 200 µl final reaction mixture. The reaction was stopped after 24 h by adding 1 ml of 0.5 M Na_2CO_3/$NaHCO_3$, pH 10.7, and read at 460 nm using a VersaFluor Fluorometer (Bio-Rad Laboratories). The activities were expressed as nanometers/hour/milligram.

Western blotting and biochemical analysis. Total cell lysates were obtained in RIPA buffer (50 mM Tris, 250 mM NaCl, 0.1% SDS, 0.5 Na-deoxycholate, and 1% NP-40). Total protein (50 µg) from each lysate was subjected to SDS-PAGE under reducing conditions. After electrophoresis, the protein was transferred onto nitrocellulose filter membranes (Immobilon-P; Millipore) using a Trans-Blot Cell (Bio-Rad Laboratories) and transfer buffer containing 25 mM Tris, 192 mM glycine, and 20% methanol. The membranes were then placed in 5% nonfat milk in TBS plus 0.5% Tween 20 (TBST) at 4°C for 2 h, to block nonspecific binding sites. The filters were incubated with specific antibodies before being washed three times in TBST and then incubated with a peroxidase-conjugated secondary antibody (GE Healthcare). After further washing in TBST, peroxidase activity was detected using the ECL system (Thermo Fisher Scientific).

RNA extraction and real-time RT-PCR. Total RNA was extracted from WT and *Sumf1*$^{-/-}$ HSPCs using the Agilent Total RNA Isolation Micro kit 50 (Agilent Technologies), according to the manufacturer protocol. The eluted RNA was reverse-transcribed with SuperScript III (Invitrogen) according to the manufacturer protocol. Quantitative real-time PCR reactions were set up in duplicate using Platinum SYBR Green qPCR SuperMix-UDG with ROX (Invitrogen), and amplification was performed using a 7,000 ABI Real-Time PCR machine. Real-time PCR was performed using 12.5 µl SYBR green Master Mix, 2.5 µl of each primer (10 µM each), and DNase- and RNase-free water for a final reaction volume of 25 µl, with the following parameters: 95°C for 3 min, followed by 40 cycles of 95°C for 10 s, 60°C for 20 s, and 72°C for 10 s. Primers were designed using PrimerExpress software (Applied Biosystems). Data analyses were performed using the Applied Biosystems SDS software, version 1.2.3. All experiments were performed in triplicate, and differences in cDNA input were "compensated" for by normalization to expression of *GAPDH*. The primers used were as follows: *Axin2* primers mix (SuperArray Bioscience Corporation); GATA-1 primers mix (SuperArray Bioscience Corporation); *GPC3* primers mix (SuperArray Bioscience Corporation); Hes-1 (forward) 5′-AAAGCCTATCATGGAGAAGAGGCG-3′ and (reverse) 5′-GGAATGCCGGGAGCTATCTTTCTT-3′; *Notch1*, (forward) 5′-GCAGCCACAGAACTTACCACTCCAG-3′ and (reverse) 5′-TAAATGCCTCTGGAATGTGGGTGAT-3′; Deltex-1, (forward) 5′-GCCATGTACTCCAATGGCAACAAG-3′ and (reverse) 5′-CGGGATGAGGTGAAACTCCATCTT-3′; C/EBPα, (forward) 5′-GGCGGCATCTGCGAGCACGA-3′ and (reverse) 5′-GGCTGTGCTGGAAGAGGTCG-3′; *GAPDH*, (forward) 5′-ACTCCCACTCTTCCACCTTC-3′ and (reverse) 5′-TCTTGCTCAGTGTCCTTGC-3′.

SU5402 bead preparation and mice treatment. 50 µl of packed AG1-2X resin (Bio-Rad Laboratories) was incubated in the presence of 500 µM SU5402 (Calbiochem) for 1 h at room temperature. The suspension was than centrifuged to remove the excess SU5402, washed twice in PBS, and resuspended in 100 µl PBS, for i.p. injection.

Gating strategies. Gating strategies for stem cells and progenitors were applied according to the Weissman Laboratory protocol (Irving L. Weissman, Institute of Stem Cell Biology and Regenerative Medicine, Stanford Cancer Center, Stanford University School of Medicine, Stanford, CA). In brief, the following populations were identified: KLS, staining was performed on lineage-selected cells, with KLS cells defined as c-kit$^+$, Sca1$^+$; CLPs, staining was performed on lineage-selected cells, with CLP cells defined as c-kit$^+$, Sca1$^+$, CD127$^+$; CMPs, staining was performed on lineage-selected cells, with CMP cells defined as c-kit$^+$, Sca1$^-$, CD127$^-$, Cd34$^+$, CD16^{low}; MEPs, staining was performed on lineage-selected cells, with MEPs defined as c-kit$^+$, Sca1$^-$, CD127$^-$, CD34$^-$, CD16$^{+/low}$; GMPs, staining was performed on lineage-selected cells, with GMPs defined as c-kit$^+$, Sca1$^-$, CD127$^-$, Cd34$^+$, CD16^{high}; pro–B cells, staining was performed on total BM, with pro–B cells defined as B220$^{+/low}$, IgM$^-$, CD127$^+$; immature B cells, staining was performed on total BM, with immature B cells defined as B220$^{+/low}$, IgM$^+$; mature B cells, staining was performed on total BM, with mature B cells defined as B220^{bright}, IgM$^{+/-}$; pro–T cells, staining was performed on total BM, with pro–T cells defined as CD127$^+$, CD3, CD4, CD8$^{-/low}$, CD25$^-$, c-kit$^+$.

Clonogenic assay. Colony-forming assays were performed by plating 5×10^3 untransduced or transduced, WT, and *Sumf1*$^{-/-}$ HSPCs in methylcellulose medium (mouse MethoCult; Stem Cell Technologies) supplemented with cytokines. After 1 wk, the colonies were scored under light or fluorescence microscopy, to evaluate the percentages of GFP$^+$ cells.

Online supplemental material. Fig. S1 shows the Western blot analysis of phospho-FSR2 and (Glypican 3) *GPC3* mRNA in WT and *Sumf1*$^{-/-}$ HSPCs. Fig. S2 shows *GATA-1* and *c/EBP*α mRNA expression in WT and *Sumf1*$^{-/-}$ HSPCs. Fig. S3 shows the analysis of BM, spleen, and thymus cellularity in WT, *Sumf1*$^{-/-}$, *Ids*$^{-/-}$, *Sulf1*$^{-/-}$, and *Sulf2*$^{-/-}$ mice. Fig. S4 shows analysis of the erythroid lineage in *Ids*$^{-/-}$, *Sulf1*$^{-/-}$, and *Sulf2*$^{-/-}$ mice. Fig. S5 shows analysis of lymphoid lineage in *Ids*$^{-/-}$, *Sulf1*$^{-/-}$, and *Sulf2*$^{-/-}$ models. Online supplemental material is available at http://www.jem.org/cgi/content/full/jem.20091022/DC1.

The authors thank A. Baldini, A. Ballabio, G. Diez-Roux and C. Settembre for critical reading of the manuscript, X. Ai for comments on the manuscript and for providing the *Sulf1*$^{-/-}$ *Sulf2*$^{-/-}$ mice, C. Procaccini and G. Matarese for useful suggestions on the experiments, B. Gentner for precious suggestions and help in the cytofluorimetric analysis, and L. Mele for technical support.

We are grateful for financial support from the Telethon Foundation (M.P. Cosma and A. Biffi) and from Associazione Italiana Ricerca sul Cancro (M.P. Cosma).

The authors declare that they have not competing financial interests.

Submitted: 8 May 2009
Accepted: 4 June 2010

REFERENCES

Ai, X., A.T. Do, O. Lozynska, M. Kusche-Gullberg, U. Lindahl, and C.P. Emerson Jr. 2003. QSulf1 remodels the 6-O sulfation states of cell surface heparan sulfate proteoglycans to promote Wnt signaling. *J. Cell Biol.* 162:341–351. doi:10.1083/jcb.200212083

Akashi, K., D. Traver, T. Miyamoto, and I.L. Weissman. 2000. A clonogenic common myeloid progenitor that gives rise to all myeloid lineages. *Nature.* 404:193–197. doi:10.1038/35004599

Anton, R., H.A. Kestler, and M. Kühl. 2007. Beta-catenin signaling contributes to stemness and regulates early differentiation in murine embryonic stem cells. *FEBS Lett.* 581:5247–5254. doi:10.1016/j.febslet.2007.10.012

Austin, T.W., G.P. Solar, F.C. Ziegler, L. Liem, and W. Matthews. 1997. A role for the Wnt gene family in hematopoiesis: expansion of multilineage progenitor cells. *Blood.* 89:3624–3635.

Baba, Y., K.P. Garrett, and P.W. Kincade. 2005. Constitutively active beta-catenin confers multilineage differentiation potential on lymphoid and myeloid progenitors. *Immunity*. 23:599–609. doi:10.1016/j.immuni.2005.10.009

Bafico, A., G. Liu, A. Yaniv, A. Gazit, and S.A. Aaronson. 2001. Novel mechanism of Wnt signalling inhibition mediated by Dickkopf-1 interaction with LRP6/Arrow. *Nat. Cell Biol.* 3:683–686. doi:10.1038/35083081

Batard, P., M.N. Monier, N. Fortunel, K. Ducos, P. Sansilvestri-Morel, T. Phan, A. Hatzfeld, and J.A. Hatzfeld. 2000. TGF-(beta)1 maintains hematopoietic immaturity by a reversible negative control of cell cycle and induces CD34 antigen up-modulation. *J. Cell Sci.* 113:383–390.

Bejsovec, A. 2005. Wnt pathway activation: new relations and locations. *Cell*. 120:11–14.

Bhardwaj, G., B. Murdoch, D. Wu, D.P. Baker, K.P. Williams, K. Chadwick, L.E. Ling, F.N. Karanu, and M. Bhatia. 2001. Sonic hedgehog induces the proliferation of primitive human hematopoietic cells via BMP regulation. *Nat. Immunol.* 2:172–180. doi:10.1038/84282

Biffi, A., M. De Palma, A. Quattrini, U. Del Carro, S. Amadio, I. Visigalli, M. Sessa, S. Fasano, R. Brambilla, S. Marchesini, et al. 2004. Correction of metachromatic leukodystrophy in the mouse model by transplantation of genetically modified hematopoietic stem cells. *J. Clin. Invest.* 113:1118–1129.

Blank, U., G. Karlsson, and S. Karlsson. 2008. Signaling pathways governing stem-cell fate. *Blood*. 111:492–503. doi:10.1182/blood-2007-07-075168

Cardone, M, V.A. Polito, S. Pepe, L. Mann, A. D'Azzo, A. Auricchio, A. Ballabio, and M.P. Cosma. 2006. Correction of Hunter syndrome in the MPSII mouse model by AAV2/8-mediated gene delivery. *Hum. Mol. Genet.* 15:1225–1236.

Clevers, H., B. Alarcon, T. Wileman, and C. Terhorst. 1988. The T cell receptor/CD3 complex: a dynamic protein ensemble. *Annu. Rev. Immunol.* 6:629–662. doi:10.1146/annurev.iy.06.040188.003213

Cobas, M., A. Wilson, B. Ernst, S.J. Mancini, H.R. MacDonald, R. Kemler, and F. Radtke. 2004. β-catenin is dispensable for hematopoiesis and lymphopoiesis. *J. Exp. Med.* 199:221–229. doi:10.1084/jem.20031615

Cosma, M.P., S. Pepe, I. Annunziata, R.F. Newbold, M. Grompe, G. Parenti, and A. Ballabio. 2003. The multiple sulfatase deficiency gene encodes an essential and limiting factor for the activity of sulfatases. *Cell*. 113:445–456. doi:10.1016/S0092-8674(03)00348-9

Cosma, M.P., S. Pepe, G. Parenti, C. Settembre, I. Annunziata, R. Wade-Martins, C. Di Domenico, P. Di Natale, A. Mankad, B. Cox, et al. 2004. Molecular and functional analysis of SUMF1 mutations in multiple sulfatase deficiency. *Hum. Mutat.* 23:576–581. doi:10.1002/humu.20040

Deftos, M.L., E. Huang, E.W. Ojala, K.A. Forbush, and M.J. Bevan. 2000. Notch1 signaling promotes the maturation of CD4 and CD8 SP thymocytes. *Immunity*. 13:73–84. doi:10.1016/S1074-7613(00)00009-1

Dhoot, G.K., M.K. Gustafsson, X. Ai, W. Sun, D.M. Standiford, and C.P. Emerson Jr. 2001. Regulation of Wnt signaling and embryo patterning by an extracellular sulfatase. *Science*. 293:1663–1666. doi:10.1126/science.293.5535.1663

Dierks, T., B. Schmidt, L.V. Borissenko, J. Peng, A. Preusser, M. Mariappan, and K. von Figura. 2003. Multiple sulfatase deficiency is caused by mutations in the gene encoding the human C(alpha)-formylglycine generating enzyme. *Cell*. 113:435–444. doi:10.1016/S0092-8674(03)00347-7

Ding, Q., W. Xia, J.C. Liu, J.Y. Yang, D.F. Lee, J. Xia, G. Bartholomeusz, Y. Li, Y. Pan, Z. Li, et al. 2005. Erk associates with and primes GSK-3beta for its inactivation resulting in upregulation of beta-catenin. *Mol. Cell*. 19:159–170. doi:10.1016/j.molcel.2005.06.009

Duncan, A.W., F.M. Rattis, L.N. DiMascio, K.L. Congdon, G. Pazianos, C. Zhao, K. Yoon, J.M. Cook, K. Willert, N. Gaiano, and T. Reya. 2005. Integration of Notch and Wnt signaling in hematopoietic stem cell maintenance. *Nat. Immunol.* 6:314–322. doi:10.1038/ni1164

Esko, J.D., and U. Lindahl. 2001. Molecular diversity of heparan sulfate. *J. Clin. Invest.* 108:169–173.

Fleming, H.E., V. Janzen, C. Lo Celso, J. Guo, K.M. Leahy, H.M. Kronenberg, and D.T. Scadden. 2008. Wnt signaling in the niche enforces hematopoietic stem cell quiescence and is necessary to preserve self-renewal in vivo. *Cell Stem Cell*. 2:274–283. doi:10.1016/j.stem.2008.01.003

Fraldi, A., K. Hemsley, A. Crawley, A. Lombardi, A. Lau, L. Sutherland, A. Auricchio, A. Ballabio, and J.J. Hopwood. 2007. Functional correction of CNS lesions in an MPS-IIIA mouse model by intracerebral AAV-mediated delivery of sulfamidase and SUMF1 genes. *Hum. Mol. Genet.* 16:2693–2702.

Heavey, B., C. Charalambous, C. Cobaleda, and M. Busslinger. 2003. Myeloid lineage switch of Pax5 mutant but not wild-type B cell progenitors by C/EBPalpha and GATA factors. *EMBO J.* 22:3887–3897. doi:10.1093/emboj/cdg380

Holst, C.R., H. Bou-Reslan, B.B. Gore, K. Wong, D. Grant, S. Chalasani, R.A. Carano, G.D. Frantz, M. Tessier-Lavigne, B. Bolon, et al. 2007. Secreted sulfatases Sulf1 and Sulf2 have overlapping yet essential roles in mouse neonatal survival. *PLoS One*. 2:e575. doi:10.1371/journal.pone.0000575

Hoppler, S., and C.L. Kavanagh. 2007. Wnt signalling: variety at the core. *J. Cell Sci.* 120:385–393. doi:10.1242/jcs.03363

Hopwood, J.J., and A. Ballabio. 2001. Multiple sulfatase deficiency and the nature of the sulfatase family. *In* The metabolic and molecular basis of inherited disease. Vol. 3. C.R. Scriver, A.L. Beaudet, D. Valle, and W.S. Sly, editors. Mc Graw-Hill, New York. p. 3725-3732.

Huang, Z., H. Xie, V. Ioannidis, W. Held, H. Clevers, M.S. Sadim, and Z. Sun. 2006. Transcriptional regulation of CD4 gene expression by T cell factor-1/beta-catenin pathway. *J. Immunol.* 176:4880–4887.

Israsena, N., M. Hu, W. Fu, L. Kan, and J.A. Kessler. 2004. The presence of FGF2 signaling determines whether beta-catenin exerts effects on proliferation or neuronal differentiation of neural stem cells. *Dev. Biol.* 268:220–231. doi:10.1016/j.ydbio.2003.12.024

Kirstetter, P., K. Anderson, B.T. Porse, S.E. Jacobsen, and C. Nerlov. 2006. Activation of the canonical Wnt pathway leads to loss of hematopoietic stem cell repopulation and multilineage differentiation block. *Nat. Immunol.* 7:1048–1056. doi:10.1038/ni1381

Kondo, M., I.L. Weissman, and K. Akashi. 1997. Identification of clonogenic common lymphoid progenitors in mouse bone marrow. *Cell*. 91:661–672. doi:10.1016/S0092-8674(00)80453-5

Kouhara, H., Y.R. Hadari, T. Spivak-Kroizman, J. Schilling, D. Bar-Sagi, I. Lax, and J. Schlessinger. 1997. A lipid-anchored Grb2-binding protein that links FGF-receptor activation to the Ras/MAPK signaling pathway. *Cell*. 89:693–702. doi:10.1016/S0092-8674(00)80252-4

Lai, J., J. Chien, J. Staub, R. Avula, E.L. Greene, T.A. Matthews, D.I. Smith, S.H. Kaufmann, L.R. Roberts, and V. Shridhar. 2003. Loss of HSulf-1 up-regulates heparin-binding growth factor signaling in cancer. *J. Biol. Chem.* 278:23107–23117. doi:10.1074/jbc.M302203200

Lai, J.P., D.S. Sandhu, C. Yu, T. Han, C.D. Moser, K.K. Jackson, R.B. Guerrero, I. Aderca, H. Isomoto, M.M. Garrity-Park, et al. 2008. Sulfatase 2 up-regulates glypican 3, promotes fibroblast growth factor signaling, and decreases survival in hepatocellular carcinoma. *Hepatology*. 47:1211–1222. doi:10.1002/hep.22202

Laiosa, C.V., M. Stadtfeld, and T. Graf. 2006a. Determinants of lymphoid-myeloid lineage diversification. *Annu. Rev. Immunol.* 24:705–738. doi:10.1146/annurev.immunol.24.021605.090742

Laiosa, C.V., M. Stadtfeld, H. Xie, L. de Andres-Aguayo, and T. Graf. 2006b. Reprogramming of committed T cell progenitors to macrophages and dendritic cells by C/EBP alpha and PU.1 transcription factors. *Immunity*. 25:731–744. doi:10.1016/j.immuni.2006.09.011

Lamanna, W.C., M.A. Frese, M. Balleininger, and T. Dierks. 2008. Sulf loss influences N-, 2-O-, and 6-O-sulfation of multiple heparan sulfate proteoglycans and modulates fibroblast growth factor signaling. *J. Biol. Chem.* 283:27724–27735. doi:10.1074/jbc.M802130200

Lluis, F., E. Pedone, S. Pepe, and M.P. Cosma. 2008. Periodic activation of Wnt/beta-catenin signaling enhances somatic cell reprogramming mediated by cell fusion. *Cell Stem Cell*. 3:493–507. doi:10.1016/j.stem.2008.08.017

Logan, C.Y., and R. Nusse. 2004. The Wnt signaling pathway in development and disease. *Annu. Rev. Cell Dev. Biol.* 20:781–810. doi:10.1146/annurev.cellbio.20.010403.113126

Michie, A.M., A.C. Chan, M. Ciofani, M. Carleton, J.M. Lefebvre, Y. He, D.M. Allman, D.L. Wiest, J.C. Zúñiga-Pflücker, and D.J. Izon. 2007. Constitutive Notch signalling promotes CD4 CD8 thymocyte

differentiation in the absence of the pre-TCR complex, by mimicking pre-TCR signals. *Int. Immunol.* 19:1421–1430. doi:10.1093/intimm/dxm113

Moon, R.T., J.D. Brown, and M. Torres. 1997. WNTs modulate cell fate and behavior during vertebrate development. *Trends Genet.* 13:157–162. doi:10.1016/S0168-9525(97)01093-7

Morimoto-Tomita, M., K. Uchimura, Z. Werb, S. Hemmerich, and S.D. Rosen. 2002. Cloning and characterization of two extracellular heparin-degrading endosulfatases in mice and humans. *J. Biol. Chem.* 277:49175–49185. doi:10.1074/jbc.M205131200

Morrison, S.J., and I.L. Weissman. 1994. The long-term repopulating subset of hematopoietic stem cells is deterministic and isolatable by phenotype. *Immunity*. 1:661–673. doi:10.1016/1074-7613(94)90037-X

Morrison, S.J., H.D. Hemmati, A.M. Wandycz, and I.L. Weissman. 1995. The purification and characterization of fetal liver hematopoietic stem cells. *Proc. Natl. Acad. Sci. USA.* 92:10302–10306. doi:10.1073/pnas.92.22.10302

Orkin, S.H., and L.I. Zon. 2008. Hematopoiesis: an evolving paradigm for stem cell biology. *Cell.* 132:631–644. doi:10.1016/j.cell.2008.01.025

Pellegrini, L., D.F. Burke, F. von Delft, B. Mulloy, and T.L. Blundell. 2000. Crystal structure of fibroblast growth factor receptor ectodomain bound to ligand and heparin. *Nature.* 407:1029–1034. doi:10.1038/35039551

Plati, T., I. Visigalli, A. Capotondo, M. Buono, L. Naldini, M.P. Cosma, and A. Biffi. 2009. Development and maturation of invariant NKT cells in the presence of lysosomal engulfment. *Eur. J. Immunol.* 39:2748–2754. doi:10.1002/eji.200939639

Prusty, D., B.H. Park, K.E. Davis, and S.R. Farmer. 2002. Activation of MEK/ERK signaling promotes adipogenesis by enhancing peroxisome proliferator-activated receptor gamma (PPARgamma) and C/EBPalpha gene expression during the differentiation of 3T3-L1 preadipocytes. *J. Biol. Chem.* 277:46226–46232. doi:10.1074/jbc.M207776200

Ratzka, A., I. Kalus, M. Moser, T. Dierks, S. Mundlos, and A. Vortkamp. 2008. Redundant function of the heparan sulfate 6-O-endosulfatases Sulf1 and Sulf2 during skeletal development. *Dev. Dyn.* 237:339–353. doi:10.1002/dvdy.21423

Reya, T., A.W. Duncan, L. Ailles, J. Domen, D.C. Scherer, K. Willert, L. Hintz, R. Nusse, and I.L. Weissman. 2003. A role for Wnt signalling in self-renewal of haematopoietic stem cells. *Nature.* 423:409–414. doi:10.1038/nature01593

Sardiello, M., I. Annunziata, G. Roma, and A. Ballabio. 2005. Sulfatases and sulfatase modifying factors: an exclusive and promiscuous relationship. *Hum. Mol. Genet.* 14:3203–3217. doi:10.1093/hmg/ddi351

Scheller, M., J. Huelsken, F. Rosenbauer, M.M. Taketo, W. Birchmeier, D.G. Tenen, and A. Leutz. 2006. Hematopoietic stem cell and multilineage defects generated by constitutive beta-catenin activation. *Nat. Immunol.* 7:1037–1047. doi:10.1038/ni1387

Schmidt, B., T. Selmer, A. Ingendoh, and K. von Figura. 1995. A novel amino acid modification in sulfatases that is defective in multiple sulfatase deficiency. *Cell.* 82:271–278. doi:10.1016/0092-8674(95)90314-3

Settembre, C., I. Annunziata, C. Spampanato, D. Zarcone, G. Cobellis, E. Nusco, E. Zito, C. Tacchetti, M.P. Cosma, and A. Ballabio. 2007. Systemic inflammation and neurodegeneration in a mouse model of multiple sulfatase deficiency. *Proc. Natl. Acad. Sci. USA.* 104:4506–4511. doi:10.1073/pnas.0700382104

Settembre, C., E. Arteaga-Solis, M.D. McKee, R. de Pablo, Q. Al Awqati, A. Ballabio, and G. Karsenty. 2008. Proteoglycan desulfation determines the efficiency of chondrocyte autophagy and the extent of FGF signaling during endochondral ossification. *Genes Dev.* 22:2645–2650. doi:10.1101/gad.1711308

Sitnicka, E., F.W. Ruscetti, G.V. Priestley, N.S. Wolf, and S.H. Bartelmez. 1996. Transforming growth factor beta 1 directly and reversibly inhibits the initial cell divisions of long-term repopulating hematopoietic stem cells. *Blood.* 88:82–88.

Spangrude, G.J., S. Heimfeld, and I.L. Weissman. 1988. Purification and characterization of mouse hematopoietic stem cells. *Science.* 241:58–62. doi:10.1126/science.2898810

Staal, F.J., and J.M. Sen. 2008. The canonical Wnt signaling pathway plays an important role in lymphopoiesis and hematopoiesis. *Eur. J. Immunol.* 38:1788–1794. doi:10.1002/eji.200738118

Teh, H.S., P. Kisielow, B. Scott, H. Kishi, Y. Uematsu, H. Blüthmann, and H. von Boehmer. 1988. Thymic major histocompatibility complex antigens and the alpha beta T-cell receptor determine the CD4/CD8 phenotype of T cells. *Nature.* 335:229–233. doi:10.1038/335229a0

Trowbridge, J.J., A. Xenocostas, R.T. Moon, and M. Bhatia. 2006. Glycogen synthase kinase-3 is an in vivo regulator of hematopoietic stem cell repopulation. *Nat. Med.* 12:89–98. doi:10.1038/nm1339

Tsai, S.F., D.I. Martin, L.I. Zon, A.D. D'Andrea, G.G. Wong, and S.H. Orkin. 1989. Cloning of cDNA for the major DNA-binding protein of the erythroid lineage through expression in mammalian cells. *Nature.* 339:446–451. doi:10.1038/339446a0

Ueno, S., G. Weidinger, T. Osugi, A.D. Kohn, J.L. Golob, L. Pabon, H. Reinecke, R.T. Moon, and C.E. Murry. 2007. Biphasic role for Wnt/beta-catenin signaling in cardiac specification in zebrafish and embryonic stem cells. *Proc. Natl. Acad. Sci. USA.* 104:9685–9690. doi:10.1073/pnas.0702859104

Utsugisawa, T., J.L. Moody, M. Aspling, E. Nilsson, L. Carlsson, and S. Karlsson. 2006. A road map toward defining the role of Smad signaling in hematopoietic stem cells. *Stem Cells.* 24:1128–1136. doi:10.1634/stemcells.2005-0263

Viviano, B.L., S. Paine-Saunders, N. Gasiunas, J. Gallagher, and S. Saunders. 2004. Domain-specific modification of heparan sulfate by Qsulf1 modulates the binding of the bone morphogenetic protein antagonist Noggin. *J. Biol. Chem.* 279:5604–5611. doi:10.1074/jbc.M310691200

Wang, S., X. Ai, S.D. Freeman, M.E. Pownall, Q. Lu, D.S. Kessler, and C.P. Emerson Jr. 2004. QSulf1, a heparan sulfate 6-O-endosulfatase, inhibits fibroblast growth factor signaling in mesoderm induction and angiogenesis. *Proc. Natl. Acad. Sci. USA.* 101:4833–4838. doi:10.1073/pnas.0401028101

Willert, K., J.D. Brown, E. Danenberg, A.W. Duncan, I.L. Weissman, T. Reya, J.R. Yates III, and R. Nusse. 2003. Wnt proteins are lipid-modified and can act as stem cell growth factors. *Nature.* 423:448–452. doi:10.1038/nature01611

Yeoh, J.S., R. van Os, E. Weersing, A. Ausema, B. Dontje, E. Vellenga, and G. de Haan. 2006. Fibroblast growth factor-1 and -2 preserve long-term repopulating ability of hematopoietic stem cells in serum-free cultures. *Stem Cells.* 24:1564–1572. doi:10.1634/stemcells.2005-0439

Yu, Q., and J.M. Sen. 2007. Beta-catenin regulates positive selection of thymocytes but not lineage commitment. *J. Immunol.* 178:5028–5034.

Zito, E., M. Buono, S. Pepe, C. Settembre, I. Annunziata, E.M. Surace, T. Dierks, M. Monti, M. Cozzolino, P. Pucci, et al. 2007. Sulfatase modifying factor 1 trafficking through the cells: from endoplasmic reticulum to the endoplasmic reticulum. *EMBO J.* 26:2443–2453. doi:10.1038/sj.emboj.7601695